C 94

Ann. Phys. Fr. **14** (1989) 49-88 FÉVRIER **1989**, PAGE 49

Antiproton-nucleus interaction

J. Cugnon and J. Vandermeulen

Université de Liège, Physique Nucléaire Théorique, Institut de Physique au Sart Tilman, Bâtiment B 5, B-4000 Liège 1, Belgium

Résumé. — Cet article constitue une revue de la physique antiproton-noyau. Du point de vue expérimental, cette revue porte particulièrement sur les récents résultats obtenus à LEAR, BNL et KEK. On y a aussi inclus une mise à jour des faits expérimentaux principaux pour $\bar{p}p$ et $\bar{p}n$. L'interaction antiproton-noyau conduit à la diffusion élastique, inélastique et d'échange de charge et à des processus d'annihilation. Habituellement, les expériences de diffusion sont analysées en termes de potentiels complexes. La relation entre ces potentiels, la conjugaison de charge et la phénoménologie de Dirac est discutée. On s'est particulièrement intéressé à la dynamique de l'annihilation d'antiprotons sur des noyaux. Le transfert d'énergie, l'absorption de pions et la réponse de la cible sont analysés dans le cadre du modèle de cascade intranucléaire. Certains autres points sont discutés plus en détail : la production d'étrangeté, la formation d'hypernoyaux et l'annihilation sur deux nucléons. On discute des signatures possibles de ce dernier processus. Enfin, la question très débattue de la formation du plasma quark-gluon est analysée.

Abstract. — The antiproton-nucleus physics is reviewed. On the experimental side, the recent results obtained at the LEAR, BNL and KEK facilities are analyzed. A brief summary of the main $\bar{p}p$ and $\bar{p}n$ experimental data is also given. The antiproton-nucleus interaction can lead to elasic, inelastic and charge exchange scattering and to annihilation. The latter is very dominant. The scattering cross-sections are usually analyzed in terms of complex potential models. The relationship between potentials, charge conjugation and Dirac phenomenology is discussed. Much emphasis is put on the dynamics of the antiproton annihilation on nuclei. The energy transfer, pion absorption and target response are analyzed within the intranuclear cascade model. Special interest is devoted to strangeness production, hypernucleus formation and possible annihilation on two nucleons. Signatures for this new process are searched in experimental data. Finally, the highly debated question of quark-gluon formation is analyzed.

1. Introduction.

The concept of antiparticle was introduced by Dirac in 1932. Soon after, the positron, the antiparticle of the electron was discovered. The next antiparticle to be discovered was the antiproton, at the Bevatron in 1955. A number of other antiparticles have been identified since and the concept of particle-antiparticle conjugation is one of the cornerstones of present fundamental theory.

When antiproton beams became available at the end of the fifties, the interaction of antiprotons became one of the subjects of elementary particle physics. Although the first experiments were made with complex targets (emulsion, heavy liquid bubble chambers), the emphasis rapidly shifted to the elementary $\bar{p}p$ interaction with the use of hydrogen bubble chamber. A number of interesting discoveries were made in the study of $\bar{p}p$ annihilations in the field of meson resonances, which are copiously produced in the annihilation. As for the interaction dynamics it appeared to be quite complicated and progress was slow.

The antiproton beams became an essential tool of high energy physics with $\bar{p}p$ CERN collider. The production of huge number of antiprotons was taken as an opportunity to build the LEAR facility for *low momentum* $\bar{p}$ beams of high intensity and excellent momentum resolution.

Since its opening in 1983 LEAR has allowed a number of studies on the $\bar{p}p$ system. It has also allowed to perform experiments with nuclear targets. Indeed, the nuclei have recently come back in high energy physics in the frame of questions on the role and properties of the subnucleonic degrees of freedom [LI88], quark-gluon plasma [Mc86a] and EMC effects [HO88]. Other antiproton beams, of however lesser quality, were available at Brookhaven and at KEK.

Slow antiprotons are potentially a new tool for hadronic and nuclear physics. In the $\bar{p}$-nucleus interaction, one can distinguish two classes of problems (which are not necessary easy to disentangle). If the annihilation process is supposed to occur on a nucleon with the same properties as in vacuum, the deposition of an energy of ~ 2 GeV with little momentum is a condition which cannot be met otherwise. Antiproton-nucleus annihilation at low energy is thus in a sense complementary to heavy ion collisions and/or other probes, for which high energy density is necessarily associated to a strong collective motion. The damage made to the nucleus may be important enough to produce new phenomena like multifragmentation, and may be controlled more easily with antiprotons than with other probes.

The second class of problems is perhaps more fundamental. Globally speaking, they have to do with the mechanism of annihilation and could also improve our understanding of charge conjugation. The $p\bar{p}$ system is the hadronic counterpart of $e^+ e^-$ for electrodynamics. Although annihilation is possible for the two systems, the properties of this phenomena for the two systems are different : $2\,\gamma$ is the most probable final state in $e^+ e^-$, whereas $5\,\pi$ (of different charges) is the most representative in $\bar{p}p$. Furthermore, only γ's are produced by $e^+ e^-$, whereas other particles besides pions can be produced in $\bar{p}p$. One is now convinced that these differences come from the composite structure of the proton. Yet, in some aspects, the charge conjugation concept plays a role in $\bar{p}p$ dynamics. However, the mechanism for the $\bar{p}p$ annihilation (see Sect. 2) is not known really. The $\bar{p}$-nucleus interaction may give some light on the $\bar{p}p$ annihilation and more generally on the $p \to \bar{p}$ charge conjugation in the presence of a nuclear medium. Conservely, one may address the question to know whether the properties of the annihilation process are modified in the presence of surrounding matter.

There is however an inherent limitation to these possibilities. As the $\bar{N}N$ cross section is very large at low momenta, essentially all the annihilations occur at the fringe of the nucleus, where the density is low. This has two consequences. Only a fraction of the annihilation products do interact with nuclear matter. The original annihilation occurs in a medium of low density.

The harvest of the first few years of LEAR experiments desserves an updating of our knowledge of the $\bar{p}$-nucleus interactions. The present paper aims at reviewing the most important results, both experimental and theoretical, and at presenting their interpretations. Our goal is not to provide definite conclusion but to emphasize the main problems and to point out the topics, for which our fundamental understanding of nuclear hadronic physics could benefit from the study of the $\bar{\mathrm{p}}$-nucleus system.

The review is organized as follows. Section 2 contains a brief account of the features of the $\bar{\mathrm{N}}\mathrm{N}$ physics, which are necessary to analyze $\bar{\mathrm{p}}$-nucleus physics. Section 3 is devoted to the study of the *interaction at rest,* i.e. of the $\bar{\mathrm{p}}$-atoms. In section 4, we discuss the main aspects of the $\bar{\mathrm{p}}$-nucleus interaction in flight, paying more attention to the annihilation process. In particular, we discuss the importance of this phenomenon for nuclear physics. Section 5 contains a discussion of special aspects, which are intensively discussed nowadays : hypernucleus formation, annihilation on two nucleons and formation of quark-gluon plasma. Finally, section 6 contains our conclusion.

2. The $\bar{\mathrm{N}}\mathrm{N}$ interaction.

2.1 General behaviour of $\bar{\mathrm{N}}\mathrm{N}$ cross-sections. — The $\bar{\mathrm{N}}\mathrm{N}$ interaction at low momentum is dominated by the strong coupling to the annihilation channels

$$\bar{\mathrm{N}}\mathrm{N} \to \text{mesons}\,. \tag{2.1}$$

The elastic scattering is then basically shadow scattering. The elastic and total cross-sections are reasonably well approximated by the strong absorption model or by a boundary condition model with $R \approx 1$ fm [DE78]. Charge exchange

$$\bar{\mathrm{p}}\mathrm{p} \to \bar{\mathrm{n}}\mathrm{n} \tag{2.2}$$

starts at $p_{\mathrm{lab}} = 0.1$ GeV/c and the cross-section rapidly reaches a broad maximum of ≈ 15 mb near $p_{\mathrm{lab}} = 0.3$ GeV/c and then regularly decreases. The $\bar{\mathrm{p}}\mathrm{n}$ total cross-section is about 10 % lower than the $\bar{\mathrm{p}}\mathrm{p}$ one [AR87] (see Sect. 2.2).

The inelastic channels of the production type, i.e. those where there is a nucleon and an antinucleon in the final state, mainly

$$\bar{\mathrm{N}}\mathrm{N} \to \bar{\mathrm{N}}\mathrm{N} + \text{mesons} \tag{2.3}$$

have their first threshold at 0.79 GeV/c. Their contribution regularly increases with energy. We call σ_{Y} the cross-section for inelastic processes leading to a final state containing an hyperon and/or an antihyperon. It corresponds to either

$$\bar{\mathrm{N}}\mathrm{N} \to \bar{\mathrm{Y}}\mathrm{Y}\,(+\,\text{mesons})\,, \tag{2.4a}$$

or

$$\bar{\mathrm{N}}\mathrm{N} \to \mathrm{N}\bar{\mathrm{N}}^*\ (\text{or } \mathrm{N}^*\bar{\mathrm{N}}),\ \bar{\mathrm{N}}^* \to \bar{\mathrm{Y}}\bar{\mathrm{K}}\ (\text{or } \mathrm{N}^* \to \mathrm{YK}) \tag{2.4b}$$

processes. The cross-section σ_{Y} increases from the $\Lambda\bar{\Lambda}$ threshold at $p_{\mathrm{lab}} = 1.43$ GeV/c to reach 1 mb near 5 GeV/c.

The variation of the various cross-sections is shown in figure 1. We derived simple parametrizations for these cross-sections (in mb) as functions of the lab momentum p (in GeV/c). We have, with obvious notation

$$\sigma_{\mathrm{ANN}} = \frac{24}{p^{1.1}} + \frac{38}{p^{0.5}} \tag{2.5a}$$

$$\begin{aligned} \sigma_{\mathrm{CEX}} &= 10.9 \frac{p-0.1}{p^{1.6}}, p < 0.5 , \\ &= 7.1\, p^{-0.9}, p > 0.5 , \end{aligned} \tag{2.5b}$$

$$\sigma_{\mathrm{EL}} = 42.3\, p^{-0.54} + 4.3 \exp[-(p-1.5)^2] , \tag{2.5c}$$

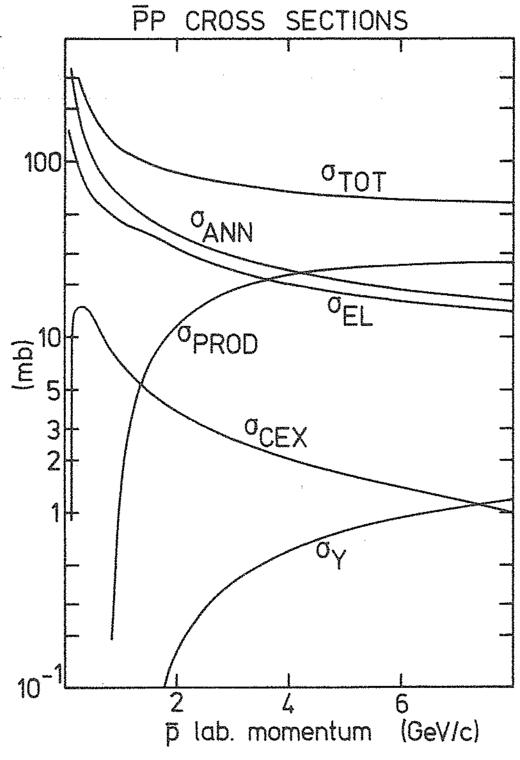

Fig. 1. — Variation of the $\bar{\mathrm{p}}\mathrm{p}$ cross-sections as a function of the $\bar{\mathrm{p}}$ lab. momentum : total σ_{TOT}, annihilation σ_{ANN}, elastic σ_{EL}, charge exchange σ_{CEX}, production (channels with a nucleon and an antinucleon in the final state) σ_{PROD}, strange production (channels with at least one hyperon (antihyperon)) σ_{Y}. The annihilation cross-section contains the $\mathrm{K}\bar{\mathrm{K}}\mathrm{n}\pi$ channels. The curves have been drawn through the data of compilation [FL84] and from some more recent data whose source can be traced back from [AM88].

and

$$\sigma_{\mathrm{PROD}} = 30 \frac{(p - 0.793)^{3/2}}{2 + (p - 0.793)^{3/2}}, \tag{2.5d}$$

and

$$\sigma_{\mathrm{Y}} = 3 \frac{(p - 1.435)}{10 + (p - 1.435)}, \tag{2.5e}$$

for non-strange and strange productions, respectively.

2.2 ANALYSIS OF THE CROSS-SECTIONS. — We give a very brief account of the potential model approaches to the $\bar{\mathrm{N}}\mathrm{N}$ system at low momentum. The usual procedure is to start from a semi-microscopic NN potential in terms of one-boson exchanges, to transform it to a real contribution by G-parity transformation and to add a phenomenological potential accounting for annihilation (which is absent in NN) [BR68]. A complex annihilation potential has been used by Dover and Richard [DO80] while a pure imaginary but strongly spin-dependent one has been used by the Paris group [CO82]. Recently, the imaginary potential has been interpreted [KO86] as the result of the convolution of the baryon (antibaryon) density distributions which give a shorter range for the imaginary part. The potential models generally provide good fits to the $\bar{\mathrm{N}}\mathrm{N}$ cross-sections in the low momentum range ($p_{\mathrm{lab}} \lesssim 1$ GeV/c). The difference between total $\bar{\mathrm{n}}\mathrm{p}$ (or $\bar{\mathrm{p}}\mathrm{n}$) and $\bar{\mathrm{p}}\mathrm{p}$ cross-sections is understood [DO86] as coming from a strong attraction in $I = 0$ channel due to coherence of several exchanges.

Let us notice that some potential models, as well as some coupled channel approaches [TI84, DA84] predict the existence of narrow resonant $\bar{\mathrm{N}}\mathrm{N}$ states and sometimes of baryonium states. There is no experimental evidence for these [AM87].

2.3 GENERAL FEATURES OF THE $\bar{\mathrm{N}}\mathrm{N}$ ANNIHILATION.

2.3.1 *Rates for annihilation at rest.* — This kind of annihilation follows the capture of a $\bar{\mathrm{p}}$ on a Bohr orbit around a proton. The stable mesons in the final state (2.1) are π, η and K ($\bar{\mathrm{K}}$) mesons, which are quite often produced *via* resonances. In annihilation at rest, ≈ 5 % of the events produce a $\mathrm{K}\bar{\mathrm{K}}$ pair, generally associated with pions (about 2 in the average [BA64, BA66]). The non-strange $\bar{\mathrm{p}}\mathrm{p}$ annihilation measured in liquid hydrogen produces a mean number $\langle n_{\pm} \rangle = 3.05$ of charged pions per annihilation [GH74]; the number of neutral pions, not directly detected, has been determined by a rather elaborate kinematical fit [GH74] and found to be $\langle n_0 \rangle = 1.96 \pm 0.23$. (However, a reanalysis [MO75] gave $\langle n_0 \rangle \approx 1.80$.) The procedure did not take account of η production. The excess $R = \langle n_0 \rangle / \langle n_+ \rangle \approx 1.15 - 1.30$ of neutral pions is also present in flight [ST79] where $R \approx 1.10 - 1.20$. An explanation may be found in terms of η production, which is generally not separated in the analyses. The η decay produces, on the average, 0.83 γ, 1.19 π^0, 0.29 π^+ and 0.29 π^-. In a bubble chamber, a γ can be mistaken for a π^0. Let the average $\bar{\mathrm{p}}\mathrm{p}$ annihilation give

$$\bar{\mathrm{p}}\mathrm{p} \to \langle \mathrm{N}_+ \rangle\, \pi^+ + \langle \mathrm{N}_0 \rangle\, \pi^0 + \langle \mathrm{N}_- \rangle\, \pi^- + \langle \mathrm{M} \rangle\, \eta\,. \tag{2.6}$$

Assuming

$$\langle N_+ \rangle = \langle N_0 \rangle = \langle N_- \rangle = \frac{\langle N \rangle}{3}, \tag{2.7}$$

we are let to the constraint

$$\frac{2}{3}\langle N \rangle + 2 \times 0.29 \times \langle M \rangle = \langle n_+ \rangle + \langle n_- \rangle \tag{2.8}$$

where $\langle n_\pm \rangle$ refer to the asymptotic pion abundances. Denoting by $\langle n_0 \rangle$ the sum of true neutral pions and γ's (which can be associated with the « observed » π^0's in bubble chamber), one can write

$$\langle n_0 \rangle = \langle N_0 \rangle + (1.19 + 0.83)\langle M \rangle . \tag{2.9}$$

Values of $\langle n_0 \rangle$, for several values of $\langle M \rangle$ are given in table I. Recent measurements [CH88] yield $\langle M \rangle = 0.07 \pm 0.01$ at rest, whereas for annihilation in flight $\langle p \rangle \approx 0.5$ GeV/c), an upper limit ($\langle M \rangle < 0.18$ with 90 % confidence [LE80]) only exists. From these figures, it seems that η production is only a partial explanation to the *neutral pion* excess.

TABLE I. — *Values of* $\langle n_\pm \rangle$ *and* $\langle n_0 \rangle$ *from equations (2.8), (2.9).*

$\langle M \rangle$	$\langle N \rangle$	$\langle n_0 \rangle$	$\langle n_\pm \rangle$	R
0.05	4.53	1.61	1.52	1.06
0.10	4.49	1.70	1.53	1.11
0.15	4.44	1.78	1.52	1.17
0.20	4.40	1.87	1.52	1.23

The production of resonances in the annihilation is well established. For instance, the rate of ω production is quite high : 0.3 ± 0.1 [LE80]. This feature, as well as η production has not been paid attention in models for $\bar{p}$-nucleus interaction.

Tables II-V give the production rates for some final channels in $\bar{p}p$ and $\bar{p}n$ (extracted from $\bar{p}d$) at rest.

2.3.2 *Rates for annihilations in flight.* — For the non-strange $\bar{p}p$ annihilations, the distribution of the number n of produced pions is pretty well described by a Gaussian form. For c.m. energy $\sqrt{s} \lesssim 30$ GeV [ST79], the parameters are given by (s in GeV^2)

$$\langle n \rangle = 2.65 + 4.10 \log_{10} s \tag{2.10}$$

$$\frac{\sigma^2}{\langle n \rangle} = 0.174\, s^{0.20} . \tag{2.11}$$

The fraction of strange annihilations increases from ≈ 5 % at rest to ≈ 10 % at a few GeV/c.

TABLE II. — *Pionic channel rates (in %) in $\bar{p}p$ at rest.*

	(a)	(b)
all neutrals	$4.1^{+0.2}_{-0.6}$	3.3 ± 0.5
$\pi^+\pi^-$	0.37 ± 0.03	0.34 ± 0.03
$\pi^+\pi^-\pi^0$	7.0 ± 0.35	8.2 ± 0.9
$\pi^+\pi^-$ MM	36.2 ± 0.8	36.2 ± 1.2
$2\pi^+ 2\pi^-$	7.0 ± 0.6	6.1 ± 0.3
$2\pi^+ 2\pi^- \pi^0$	19.8 ± 0.7	19.6 ± 0.9
$2\pi^+ 2\pi^-$ MM	21.1 ± 0.7	22.3 ± 1.1
$3\pi^+ 3\pi^-$	2.1 ± 0.2	2.0 ± 0.2
$3\pi^+ 3\pi^- \pi^0$	1.9 ± 0.2	1.7 ± 0.3
$3\pi^+ 3\pi^-$ MM	0.3 ± 0.1	0.3 ± 0.1
$\langle n_+ \rangle + \langle n_- \rangle$	3.05	3.05

MM means a neutral system $\geq 2\pi^0$. Column (a) and (b) are respectively CERN and Columbia results compiled by Armenteros *et al.* [AR80]. We have renormalized the figures to 100 % of pionic annihilations.

TABLE III. — *Pionic channel rates (in %) in $\bar{p}n$ at rest.*

	(a)	(b)
$\pi^-\pi$	< 0.7	0.75 ± 0.15
π^- MM	16.4 ± 0.5	16.9 ± 0.7
$2\pi^-\pi^+$	1.57 ± 0.21	2.3 ± 0.3
$2\pi^-\pi^+\pi^0$	21.8 ± 2.2	17 ± 2
$2\pi^-\pi^+$ MM	36.3 ± 2	39.7 ± 2
$3\pi^- 2\pi^+$	5.2 ± 0.5	4.2 ± 0.2
$3\pi^- 2\pi^+ \pi^0$	15.1 ± 1.0	12 ± 1
$3\pi^- 2\pi^+$ MM	3.3 ± 1	6.6 ± 1
7 prongs	0.39 ± 0.07	0.35 ± 0.03
$\langle n_- \rangle$	2.07	2.06
$\langle n_+ \rangle$	1.08	1.06

Data taken from (a) [BE67], (b) Syracuse results quoted in [OR73].

TABLE IV. — *Frequency (in %) distribution of the pion multiplicity for* $\bar{p}p \to n_\pi$ *at rest* [GH74].

n_π	frequency
2	0.4 ± 0.03
3	7.8 ± 0.4
4	17.5 ± 3.0
5	45.8 ± 3.0
6	22.1 ± 1.5
7	6.1 ± 1.0
8	0.3 ± 0.1
$\langle n_\pi \rangle$	5.01 ± 0.23

TABLE V. — *Partial rates for* $\bar{p}p \rightarrow K\bar{K}\, n_\pi$ *at rest in liquid hydrogen (in* 10^{-3} *of all annihilations). Same sources as for table II.*

	(a)	(b)
$K^+ K^-$	1.1 ± 0.1	0.96 ± 0.08
$K_S K_L$	0.71 ± 0.10	0.80 ± 0.05
$K_S K_S \pi^0 + K_L K_L \pi^0$	1.46 ± 0.20	1.56 ± 0.12
$K_S K_S n\pi^0$ (n > 1)	0.64 ± 0.08	0.71 ± 0.08
$K^0 K^\pm \pi^\mp$	4.25 ± 0.55	4.25 ± 0.20
$K_S K_S \pi^+ \pi^-$	2.01 ± 0.26	1.95 ± 0.23
$K_S K_L \pi^+ \pi^-$	2.41 ± 0.36	2.26 ± 0.45
$K_S K^\pm \pi^\mp \pi^0$	4.47 ± 0.53	4.69 ± 0.55
$K_S K_S \pi^+ \pi^- \pi^0$	1.49 ± 0.22	1.10 ± 0.14
$K_S K^\pm \pi^\mp \pi^+ \pi^-$	0.59 ± 0.08	0.71 ± 0.07
$K_S K\ 4\ \pi$	~ 0	~ 0
Σ strange		46 ± 19

2.3.3 *Momentum spectra.* — To a good approximation, the pion exclusive spectra can be fitted by assuming, for each multiplicity, a distribution following (invariant) phase space. Figure 2 shows the measured and fitted shapes for $\bar{p}p$ at rest. The shape is not much different from a Maxwell-Boltzmann

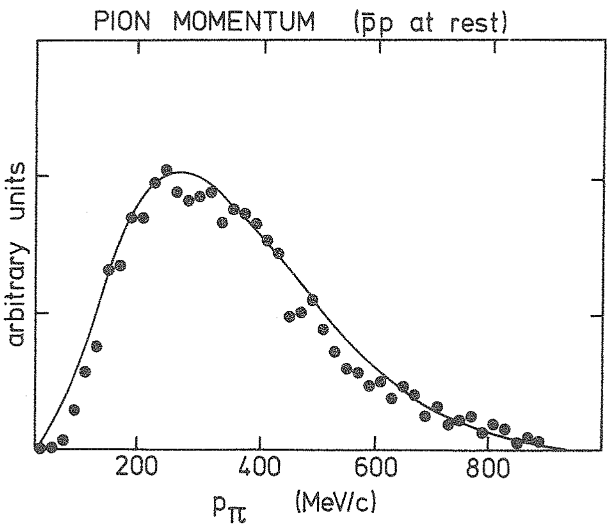

Fig. 2. — Momentum distribution of the charged pions from $\bar{p}p$ at rest ; dots : experiment [RO75] ; curve : phase space distribution.

distribution. Gregory *et al.* [GR76] have analyzed the pion spectra from annihilation in flight in terms of temperature

$$\frac{\mathrm{d}N}{pE\,\mathrm{d}E} \propto \exp(-E/T)\,; \tag{2.12}$$

they find the temperature to vary like

$$T = T_0 - C/\sqrt{s} \tag{2.13}$$

with $T_0 = 164 \pm 5$ MeV and $C = 103 \pm 15$ MeV^2. The assumption of a statistical process implies forward-backward symmetry in the c.m. Experiment does not deviate much from that property.

2.4 MODELS OF $\bar{\mathrm{N}}$N ANNIHILATION. — $\bar{\mathrm{N}}$N annihilation has been mainly tackled by statistical models and by quark models (quark rearrangement and its extensions).

2.4.1 *Statistical models.* — The application of the Fermi model to $\bar{\mathrm{N}}$N annihilation has been reviewed by Hamer [HA72] who introduced resonance production by means of the statistical bootstrap. A number of variants of this statistical model have been proposed to interpret the pion multiplicities [MÖ75, OR73, VA74, VA80, MA76]. They have basically one free parameter with the physical meaning of an interaction volume, and predict pion multiplicity shapes close to a Gaussian-like form. The underlying physical picture of fireball formation and decay is suited only for low momentum annihilations. The application of the model can be extended to intermediate energies by introducing an empirical variation of the interaction volume with energy [VA80]. Note that a satisfactory interpretation of strange annihilation requires extra parameters [CU87].

2.4.2 *Quark models.* — $\bar{\mathrm{N}}$N annihilation is expected to imply a significant overlap of the two partners and one therefore expects the quark degrees of freedom to play a crucial role. The treatment of $\bar{\mathrm{N}}$N annihilation in terms of the quark content has been initiated by the idea of the simple quark rearrangement [RU66] schematically represented on figure 3a. In this original version it is assumed that the three quarks and the three antiquarks rearrange themselves into s-wave $q\bar{q}$ pairs without exchanging spin and flavour. The channels branching ratios are obtained from rearrangement coefficients in SU_4 (spin-isospin). It was pointed out later [MA81, MA83] that it is necessary to introduce the spatial components of internal quark wavefunctions of baryons. This new version, however, introduces a number of parameters. At any rate, the main shortcoming of the quark rearrangement is its unability to accomodate two pions in the final state. An alternative scheme has therefore been introduced in terms of creation and annihilation of quark pairs. Two-meson annihilation is then discussed in terms of graphs (d) and (e) of figure 3. It has been found [FU84] that both rearrangement (a) and annihilation (b) explain with similar reliability the branching ratios for the three-meson channels while graph (e) is better than graph (d) for two-meson production. Considerable sophistication has been introduced in the treatment of $\bar{\mathrm{N}}$N annihilation in two mesons [GR88, 88a] and in three mesons [MA87],

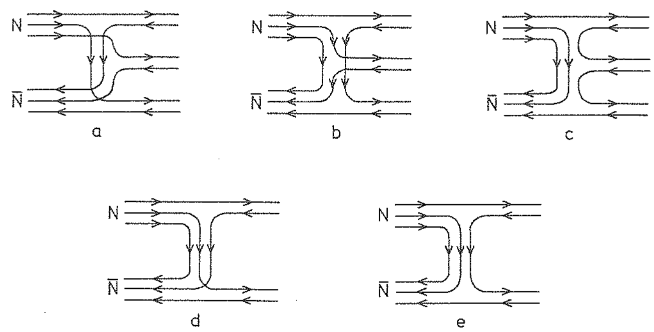

Fig. 3. — Schematic representation of quark models for N̄N annihilation : (a) rearrangement leading to three mesons, (b) and (c) annihilation leading to three mesons, (d) rearrangement and (e) annihilation, leading to two mesons.

however with presently a limitation to S-wave annihilation. The existence of selection rules in terms of the quark-gluon dynamics has been pointed out [NI85, DO86, KL88]. Presently, however, comparison with experiment is limited to a few channels. It should be realized that, as pointed out by Dover [DO86], it is difficult to experimentally separate two-body and three-body contributions, in particular if a two-body mode involves two broad mesons ; it is not excluded that two-body processes dominate N̄N annihilation. An empirical model based on this assumption, outside the quark dynamics context, and including the whole set of mesons up to 1.4 GeV has been recently proposed [VA88].

3. Interaction at rest.

3.1 INTRODUCTION. — This term designates a whole sequence of peculiar and successive aspects of the interaction between an antiproton and a nucleus. They can be enumerated and characterized as follows.

(1) A slowed down antiproton is captured in a Bohr orbit, generally with a high principal quantum number $n \sim 40$, forming so an antiprotonic atom. The latter de-excites by successive radiative transitions (the so-called electromagnetic cascade) or by Auger emission for large n. The cascade lasts for about 10^{-10} s in dense targets. This time may increase up to a microsecond in dilute gas targets.

(2) The antiprotonic atom eventually reaches a state where the antiproton wavefunction has a sufficient overlap with the nucleus for the absorption to prevail. This state is fed from the next upper one by a well-defined X-ray. The principal quantum number of this state increases with the size of the nucleus. It varies from $n = 3$ for O to $n = 9$ for Th according to [PO85]. The characteristic lifetime of the last observed bound state (the capture state) is of the order of $\sim 10^{-18}$ s.

(3) The antiproton disappears, giving birth to a few pions which start an intranuclear cascade, ejecting by collisions a few nucleons and possibly some light

particles, leaving the residual nucleus with some excitation energy. The characteristic time of this process is of the order of $\sim 10^{-22}$ s.

(4) The excitation energy is removed by ordinary channels : neutron evaporation, proton evaporation for very light nuclei and fission for heavy ones. Ultimately, the residual nucleus may emit γ-rays or β-rays, which can be used to identify it. This can also be done by looking at characteristic X-rays.

3.2 THE OBSERVABLES OF ANTIPROTONIC ATOMS. — Basically, the hydrogen-like scheme of the $\bar{p}$-atom is observed. The (relativistic) Bohr formula gives already a good account of the energy levels. The fine structure splitting $\left(j = \ell \pm \frac{1}{2}\right)$ for a $\bar{p}$-atom built on an even-even nucleus is proportional to the magnetic moment of the antiproton.

Strong interaction between the antiproton and the nucleus leads to an additional shift (ε) and to a width (Γ) of the capture state energy (it can be shown that the strong interaction effects on the other states are orders of magnitude smaller).

The values of ε and Γ have been measured for many nuclei both in the pre-LEAR era (see [PO86] for a review) and with LEAR [PO85, GO85, RO86, KÖ86, KA86, SI88]. These quantities are related to the (complex) antiproton-nucleus scattering length a through the Trueman [TR61] relation

$$\varepsilon + i\,\Gamma/2 = \frac{2(\hbar c)^2}{\mu a_0^3}\,a\,, \tag{3.1}$$

where μ is the reduced mass and a_0 the Bohr radius. The antiprotonic hydrogen is particularly interesting since it gives the $\bar{p}p$ scattering length directly and thus information on the $\bar{p}p$ interaction. The other nuclei present special interest, besides the Z and A dependence of the strong interaction effect. Studies of isotopes give information on $\bar{p}n$ (and perhaps on neutron distribution) and studies of non-zero spin targets give information on the spin-orbit part of the $\bar{p}p$ interaction. We postpone to section 3 the discussion of the physical results, since $\bar{p}$ scattering yields similar and complementary information. Let us note however that theoretical works have been devoted to the calculation of ε and Γ [HA77, NI76, SU84, DE74, KA76, DU85, GR82, GR83, WY85, WY88]. They work qualitatively well. They usually predict ε and Γ by directly calculating the bound state energies in a complex optical potential. The relation between this procedure and the Trueman relation is however not elucidated in the case of strong absorption.

3.3 THE ANTIPROTON ANNIHILATION. — Owing to the strong absorption, it is expected that the probability density decreases rapidly inside the nucleus. Indeed, in the simplest approximation, one can write

$$\Gamma = 2\,\pi \int d^3 r \int d^3 r'\, V_{\text{ann}}(|\mathbf{r} - \mathbf{r}'|)\, |\psi_{n\ell}(r)|^2\, \rho(r') \tag{3.2}$$

where V_{ann} is the annihilation potential, $\psi_{n\ell}$ is the capture state wavefunction and ρ is the nuclear density. In the zero-range approximation, one gets, now distinguishing between neutron and proton, and assuming a spherical nucleus

$$\Gamma = 8\,\pi^2 \int_0^\infty \mathrm{d}r\, r^2 |R_{n\ell}(r)|^2 \left\{V_{\mathrm{ann}}^{\bar{\mathrm{p}}\mathrm{p}}\, \rho_p(r) + V_{\mathrm{ann}}^{\bar{\mathrm{p}}\mathrm{n}}\, \rho_n(r)\right\} . \tag{3.3}$$

The integrand can be considered as the probability distribution for the distance r between the annihilation site and the center of the nucleus. This quantity is given in figure 4 [JA88] for several nuclei. (In this particular case $V_{\mathrm{ann}}^{\bar{\mathrm{p}}\mathrm{p}}$ is taken to be equal to $V_{\mathrm{ann}}^{\bar{\mathrm{p}}\mathrm{n}}$). The remarkable result is that the annihilation takes place in the outer fringes of the nucleus. In view of this result, it was expected [LE74] that this feature could be used to test the neutron distribution at the surface of the nucleus (as it was also suggested for π- and K-atoms). However, this would require a high degree of precision which lies beyond the present understanding of the phenomena since

(1) in equation (3.2), strong interaction distortion of the capture state should be taken into account. The modified $\psi_{n\ell}$ would be depleted inside the nucleus because of absorption. On the other hand, the attraction between the nucleus and the antiproton tends to drive the antiproton inside the nucleus. This effect is not precisely known (see Sect. 4) :

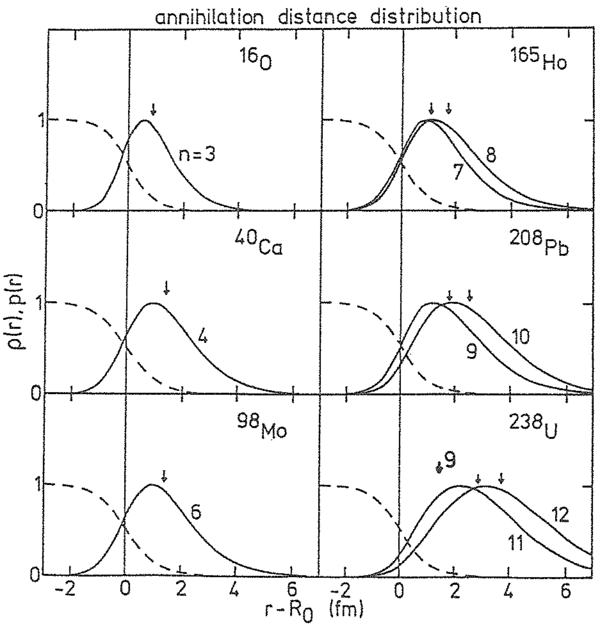

Fig. 4. — Distribution $p(r)$ of the annihilation distance r (counted from the center of the nucleus), as calculated from equation (3.3) (full curves), for various targets. The density profile is given by the dotted curve and R_0 is the half-density radius. The numbers indicate the principal quantum numbers of the annihilation state. The arrows give the average value of r. All curves are normalized on the same maximum.

(2) the difference between $V_{\mathrm{ann}}^{\bar{p}p}$ and $V_{\mathrm{ann}}^{\bar{p}n}$, i.e. the isospin dependence of the annihilation interaction, is not well known (see Sect. 2) ;

(3) it may be questionable to include the absorption distortion of ψ_{nl} in the calculation of the probability density, i.e. on the state of the system prior to absorption.

3.4 THE ANNIHILATION CHANNELS.

3.4.1 Not very much work has been devoted up to now to the study of the $\bar{p}$-nucleus annihilation channels. For the annihilation at rest, only two experiments have been performed at LEAR. In the first one (PS179), annihilations on emulsion have been studied [BA86a]. What is essentially measured is the negative pion multiplicity distribution and the charged particle multiplicity. These aspects will be discussed in section 4 with the same quantities measured for the annihilation in flight.

The second experiment (PS186) was primarily devoted to the study of the residual nucleus through its gamma radioactivity [MO86, MO86a]. The group also measured the production of ^{3}He and ^{4}He (see later) [MA88]. A typical result of the residual activity is given in figure 5, which shows that many nuclei are recorded after the $\bar{p}$-annihilation on ^{98}Mo.

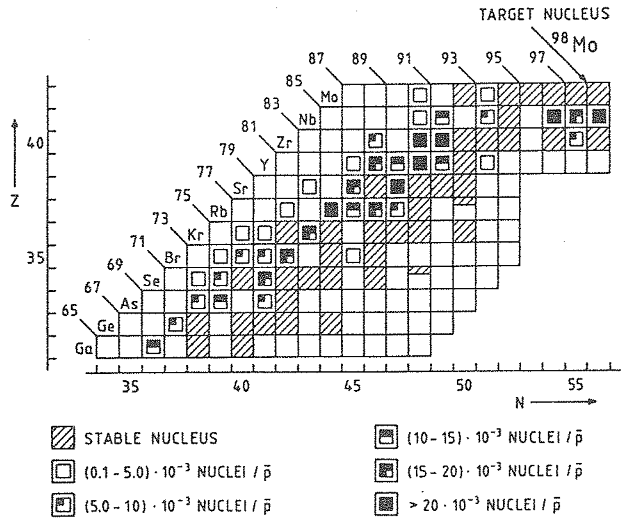

Fig. 5. — Distribution of the γ-radioactive residues measured by the PS186 experiment [MO86] after annihilation on ^{98}Mo target.

3.4.2 *The intranuclear cascade (INC) model.* — This model is essentially a simulation of the multipion cascade following the $\bar{p}$ annihilation. For the annihilation at rest, two groups have developed such a model [IL82, CU87, JA88]. The INC dynamics can be divided in three stages :

(a) the *annihilation* of the antiproton is assumed to occur on a single nucleon, with the same properties as in free space (see Sect. 2). The annihilation is supposed to occur at the fringe of the nucleus, with a probability distribution given by equation (3.2). The number of pions, and their momentum are generated according the probability laws provided by the observations of the $\bar{\text{N}}$N system (see Sect. 2) ;

(b) the *multipion* cascade. Some of the primordial pions penetrate into the nucleus, initiating the cascade process by which some of the nucleons can be ejected with large velocity. The cascade process is assumed to proceed through the following reactions

$$\text{NN} \rightleftarrows \text{NN},\ \text{NN} \rightleftarrows \text{N}\Delta,\ \Delta\Delta \rightleftarrows \Delta\Delta\,, \tag{3.4a}$$
$$\pi\text{N} \rightleftarrows \Delta\,, \tag{3.4b}$$
$$\pi\text{NN} \rightarrow \text{NN}\,, \tag{3.4c}$$
$$\pi\text{N} \rightarrow \pi\text{N},\ \pi\text{N} \rightarrow \pi\pi\text{N}\,, \tag{3.4d}$$

with probability following the experimental cross-sections. This procedure has successfully been used in heavy ion reactions in the relativistic regime (see [CU84] for a review). Reaction (3.4b) is assumed to occur in the (3, 3) resonance region, whereas (3.4c) occurs only at small energy and reactions (3.4d) are introduced above the resonance only ;

(c) the *evaporation* process. After a time span (of ~ 40 fm/c for a nucleus like Mo), the reaction rates have substantially decreased. The nucleus still contains, however, some excitation energy, which can be released by emitting particles, mainly neutrons, at a much slower pace. Usually, the INC procedure is stopped at the beginning of this stage, which is then described by conventional evaporation models. The output of such a calculation is not yet directly comparable with observations of figure 5, since they refer to two different times separated by the decay of β-unstable nuclei. The comparison can be done after correction due to this β-cascade, a procedure which has been developed in the study of the spallation reactions [RU66a].

Several aspects are generally added to this scheme : mean field (which was absent in the early version of the INC model of [CA82, CA83]), Pauli blocking, isospin degrees of freedom, etc... The two INC models mentioned above differ from each other by details only. They indeed yield very similar results, if one takes account of the uncertainty of this kind of approach.

The distribution of the residual nuclei, as predicted by the INC model [JA88], is shown in figure 6 along with the experimental distribution for two targets, ^{98}Mo and ^{165}Ho. The agreement is rather good, but several comments are in order :

(1) experimentally, events where the nucleus is left with only one nucleon less than in the target are observed. In these events, the pions emitted from the annihilation do not transfer enough energy to even evaporate a nucleon. The INC model predicts the same kind of events, with a larger rate however. In the INC picture, the primordial pions merely miss the target, because of the very peripheral location of the annihilation ;

(2) the overall agreement is noteworthy, although the INC model does not reproduce the dip for small mass loss. This may be related to a too small energy transfer ;

(3) in both cases, about one fourth of the mass loss is due to the ejection of fast nucleons by the multipion cascade and the rest is due to evaporation.

The neutrons have been detected directly in the case of the annihilation on

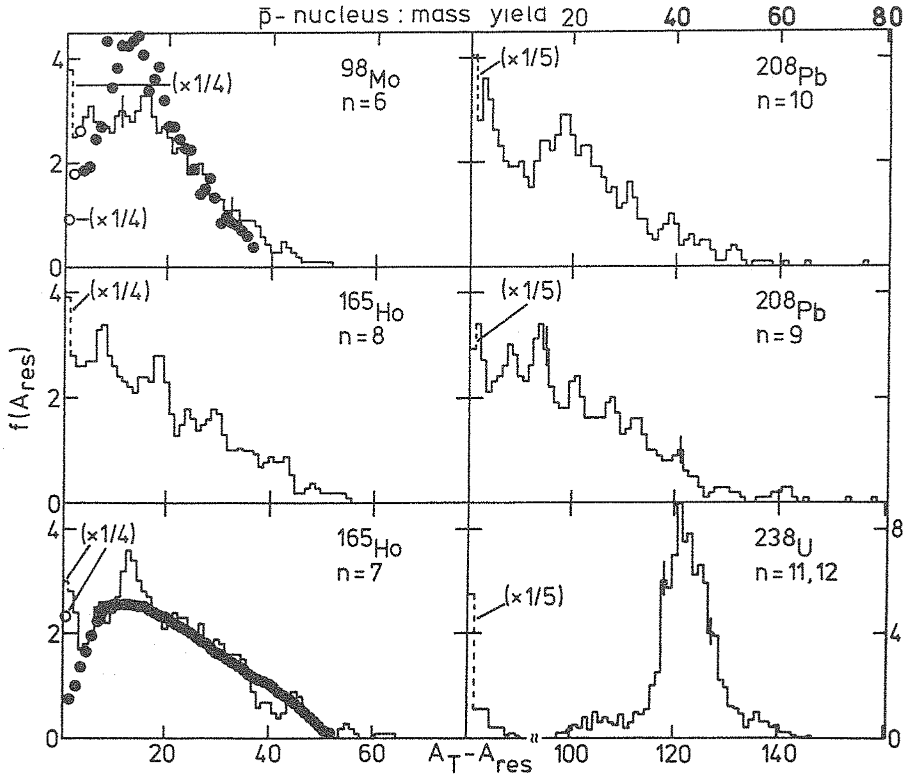

Fig. 6. — Probability distribution (in %) for the residual mass A_{res}. The histograms are the results of the INC model. The circles are the experimental data of [MO86, MO86a]. The first bin corresponds to $A_{res} = A_T - 1$, for which both the theoretical and the experimental yields are multiplied by the indicated factor. Note the broken horizontal scale and the different vertical scale for the ^{238}U case. The error bars indicate the (statistical) uncertainty of the calculation. Adapted from [JA88].

^{238}U [BÜ88], in the 100-400 MeV/c momentum range. The authors seem to have identified several components : a high energy component, which can be identified with the cascade neutrons, a *pre-equilibrium* component (which could be secondary neutrons) and a fission component. The apparent absence of evaporation is due to a competition with fission, whose probability is large in this case [JA88].

4. Interaction in flight.

4.1 INTRODUCTION. — The interaction between travelling antiprotons and nuclei takes many different forms which can be classified according to the impact parameter of the incoming antiprotons. On many aspects, this system can be paralleled with heavy ions colliding at low energy. The absorption is overwhelmingly dominant for small impact parameter and leads to decay channels very different from the incident one. For large impact parameters, the elastic scattering dominates. For a rather limited range of impact parameters corresponding to grazing collisions, one observes inelastic scattering and charge exchange $(\bar{p}, \bar{n})$ phenomena. Of course, the separation of the various impact parameter domains is less well-defined in the $\bar{p}$-nucleus case, because the relative motion is less classical than in the heavy ion case.

We will discuss each kind of reaction successively, paying more attention to the annihilation channels. We will leave some particular aspects for section 5.

4.2 INTEGRATED CROSS-SECTIONS. — The total absorption cross-section has been measured by several authors [AI81, NA84, GA84, GA85, AS84, BA86, AS85]. It shows two main properties : (1) it decreases with incident energy, which reflects the decreasing slope of the absorption $\bar{N}N$ cross-section (see Sect. 2) ; (2) it is quite large. At 180 MeV incident energy, where there are many measurements, the absorption cross-section can conveniently be described by $\sigma_R = \pi (a + r_0 A^{1/3})^2$ with $a = 0.65$ fm and $r_0 = 1.44$ fm. A similar parametrization for the p-nucleus absorption cross-section at the same energy would give roughly $a \approx -0.4$ fm, keeping the same value of r_0. This means that the nucleus is acting as a black sphere for antiprotons [VA86].

4.3 ELASTIC CROSS-SECTIONS. — Data are quite numerous, coming from LEAR [GA84, GA85, BR86], Brookhaven [AS84] and KEK [NA84]. A typical cross-section is shown in figure 7. They have been subjected to many optical-model analyses [BA84, BA85, KU85, HE85, JA85, BA86b, JA86, IN86]. All of them agree on the strong absorption nature of the $\bar{p}$-nucleus interaction. As is usual in this case (see also the heavy ion example [SA74]), the potential is unambiguously determined in the vicinity of the so-called strong absorption radius R_{abs} only, which lies a little bit outside the nuclear surface. One obtains

$$\mathrm{Re}\, V_{opt}(R_{abs}) \approx \frac{1}{2}\, \mathrm{Im}\, V_{opt}(R_{abs})\,. \tag{4.1}$$

This seems to remove the *shallow-deep* ambiguity, which was left after analysis of $\bar{p}$-atoms [WO84] : it was then found that a strongly absorptive, weakly attractive or a weakly absorptive, largely attractive potential were fitting the data. If a Woods-Saxon form

$$V_{opt} = -\frac{V_0 + iW_0}{1 + \exp \dfrac{r - \tilde{R}}{a}} \tag{4.2}$$

is assumed, then the following values are obtained from elastic scattering [JA86] :

$$\begin{aligned} V_0 &\approx 41 \text{ MeV}\,, \quad W_0 = 117 \text{ MeV} \quad \text{at} \quad p = 300 \text{ MeV/c}\,, \\ V_0 &\approx 52 \text{ MeV}\,, \quad W_0 = 145 \text{ MeV} \quad \text{at} \quad p = 600 \text{ MeV/c}\,. \end{aligned} \tag{4.3}$$

The quantity $\tilde{R}$ exceeds by ~ 0.6 fm the half-density radius, a feature which presumably follows from the range of the $\bar{N}N$ interaction. Note, however, that it is not sure that the shape would follow a Woods-Saxon form.

Analysis of the elastic scattering and, more importantly, of the polarization measurement on ^{12}C [BI85, BR85] reveals that the spin-orbit term is very small

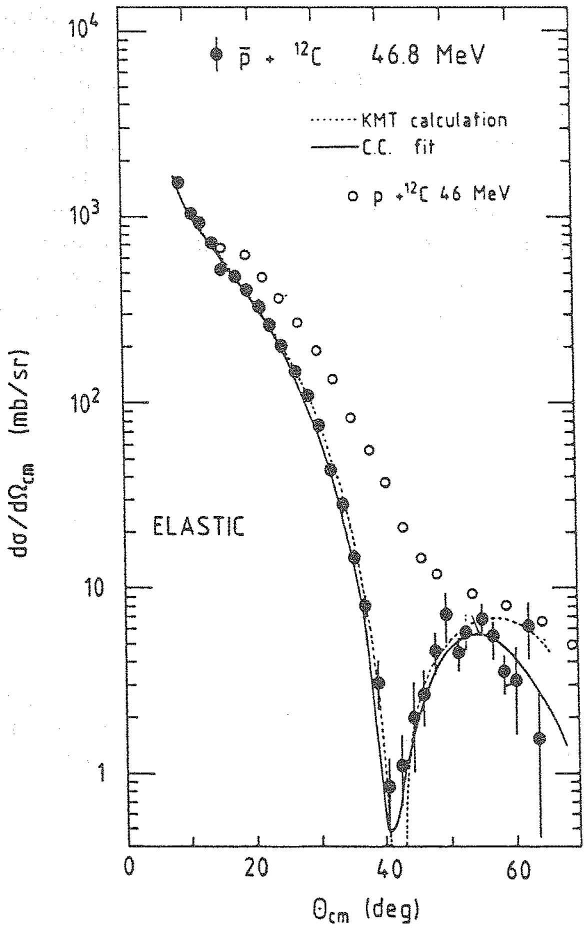

Fig. 7. — Differential cross-sections for antiproton elastic scattering from ^{12}C (solid circles). The cross-sections for proton elastic scattering are also shown for comparison (open circles). The dotted curve is a KMT calculation using the $\bar{N}N$ amplitudes of Coté *et al.* [CO82]. The solid curve results from a coupled-channel fit to the data with the following parameters : $V_0 = 25$ MeV ; $W_0 = 61$ MeV ; $r_{0v} = 1.17$ fm ; $a_v = 0.61$ fm ; $r_{0w} = 1.2$ fm ; $a_w = 0.51$ fm. From [GA84].

(compared to e.g. the p-nucleus case). Information on the isospin part of the optical-model has been tentatively extracted from $\bar{p}$ scattering by various isotopes, as well as from $\bar{p}$-atoms on various isotopes. However, no clear indication is available because the effect can be attributed as well to the modification of the density due to a neutron excess [GA85a].

The $\bar{p}$-nucleus elastic scattering has been discussed in terms of microscopic approaches, in order to clarify its relation to the $\bar{p}$-p elementary amplitudes : nonrelativistic models based on a folding of the $\bar{N}N$ potential [BO82], or of the $\bar{N}N$ free t-matrix [DO80, AD87, DA85, GR82, NI83], or of the $\bar{N}N$ medium corrected (especially by Pauli principle effects) t-matrix [vo85, AD87], on KMT formalism [GA84] and even on Glauber formalism [BA86]. Surprisingly enough, the latter two approaches yield reasonable results, which may be unexpected in view of the low incident energy. However, strong absorption may help to make Glauber type model more accurate [GA85]. Most of the microscopically constructed optical-model potentials agree more or less with experiment as for the imaginary part. The real part seems to be a delicate question. Although the $\bar{\mathrm{N}}\mathrm{N}$ potentials have a strong state dependence, the $\bar{\mathrm{N}}$-nucleus potential constructed on the t-matrix washes this structure, since it roughly corresponds to a zero-range approximation, picking up the $^{11}\mathrm{S}_0$ channel only [DO87], except if folding with non-zero range is adopted. The resulting real part is then weakly attractive, if not repulsive in the interior, because of possible medium effects [AD87].

In some works, the authors have tried to extract the $\bar{\mathrm{p}}\mathrm{n}$ scattering parameters from the $\bar{\mathrm{p}}$-nucleus cross-sections [BA87, DA88]. Roughly speaking, they observe that the $\bar{\mathrm{p}}$-n interaction is 10 to 20 % smaller than the $\bar{\mathrm{p}}\mathrm{p}$, in agreement with the measured $\bar{\mathrm{n}}\mathrm{p}$ cross-section measurement (see Sect. 2).

4.4 INELASTIC AND CHARGE-EXCHANGE REACTIONS. — The latter can be used to study the various terms of the $\bar{\mathrm{N}}\mathrm{N}$ t-matrix

$$t = t_0 + t_\sigma\, \boldsymbol{\sigma}_{\bar{\mathrm{N}}} \cdot \boldsymbol{\sigma}_{\mathrm{N}} + t_\tau\, \boldsymbol{\tau}_{\bar{\mathrm{N}}} \cdot \boldsymbol{\tau}_{\mathrm{N}} + t_{\sigma\tau}\, \boldsymbol{\sigma}_{\bar{\mathrm{N}}} \cdot \boldsymbol{\sigma}_{\mathrm{N}}\, \boldsymbol{\tau}_{\bar{\mathrm{N}}} \cdot \boldsymbol{\tau}_{\mathrm{N}} + t_{\mathrm{LS}}\, \mathbf{L} \cdot \mathbf{S} + t_{\mathrm{T}}\, S_{12}. \quad (4.4)$$

By suitably chosing the quantum numbers of the final-state, it is possible in principle to isolate a piece of this transition matrix [DO83, DO85]. In elastic scattering, everything is dominated by the central part which in any case is much larger than the other coefficients. Thus the $\Delta T = 0$, $\Delta S = 0$ natural parity excitations dominate the inelastic spectrum, when the latter has been measured. The nucleus $^{12}\mathrm{C}$ is a good candidate for the filtering procedure, since it has a 1^+ $(T = 0)$ state at 12.7 MeV and 1^+ $(T = 1)$ state at 15.1 MeV, which can be used to isolate t_σ at $t_{\sigma\tau}$, but this remains a possibility to be explored.

The $(\bar{\mathrm{p}}, \bar{\mathrm{n}})$ cross-section has been measured for $^{12}\mathrm{C}$ [NA85] and for C, Al, Cu, and Pb (at 0 degree) [BR86b]. It seems that the cross-sections are larger than what is expected from a quasi-free process (taking account of the fact that the $\bar{\mathrm{n}}$ should not be reabsorbed). The $(\bar{\mathrm{p}}, \bar{\mathrm{n}})$ reaction is potentially able to test the $t_{\sigma\tau}$ quantity and the longitudinal spin response of the nuclei ; no experimental information is available up to now.

4.5 SEARCH FOR $\bar{\mathrm{p}}$-NUCLEAR BOUND STATES. — A possible novel feature was suggested by the relativistic approach of the $\bar{\mathrm{p}}$-nucleus interaction. Since the antiproton is the antiparticle of the proton, it was appealing to understand the p-nucleus and the $\bar{\mathrm{p}}$-nucleus in a single Dirac equation. This was possible after Walecka purports the approach of the p-nucleus interaction by a Dirac equation describing the proton moving in a mean field. The latter is basically built of a scalar and a vector potentials :

$$\left\{ \gamma^\mu (p_\mu + V_\mu) + (m + S) \right\} \psi = 0 . \quad (4.5)$$

The scalar potential is attractive and the vector is repulsive. Both are very intense ($S \approx -350$ MeV, $V_0 \approx 300$ MeV) and are sometimes identified with the (average) action of the exchange of σ-mesons and ω-mesons with the target nucleons. It has been proposed that the antiparticle interacts with the nucleus through the same equation (4.5). The potentials are then to be modified by the *G*-parity transformation, which is very simple due to the meson exchange content attributed to these potentials : V changes sign, whereas S remains the same. The Dirac equation (4.5) has been shown [JA80] to be equivalent to a Schrödinger equation with central and spin-orbit terms. The depth of the central potential is given by $V + S$. The one of the spin-orbit is proportional to $V - S$. This would mean that the $\bar{\text{p}}$-nucleus central potential is very strongly attractive. Furthermore, this reasoning shows that the $\bar{\text{p}}$-nucleus spin-orbit should be much smaller than the p-nucleus one. A very strong $\bar{\text{p}}$-nucleus central potential was predicted by Duerr and Teller [DU56] already thirty years ago. This feature was reconsidered recently and shown to predict deeply bound $\bar{\text{p}}$-nucleus states (bound by the strong interaction and not by Coulomb interaction as in $\bar{\text{p}}$-atoms). We stress that this prediction heavily relies on several assumptions : (1) the proton (and the antiproton) is a Dirac particle, i.e. structureless ; (2) the interaction may be described by mean field ; (3) the fields have well-defined *G*-parity ; (4) the absorptive potential is added in an *ad hoc* fashion, without disturbing the real part.

These states have been searched for in a knock-out ($\bar{\text{p}}$, p) experiment with a spectrometer [GA85b]. The result was clearly negative, the proton spectrum being consistent with the smooth background coming from the incoherent multiple process (Sect. 5), without any signal of a $\bar{\text{p}}$-nucleus state. However, it should be noted that the kinematics used requires a very large momentum transfer for which the formation probability should be small. It has since been proposed to look at more favourable kinematics [AU86].

The phenomenologically small optical-model potential together with the negative result of reference [GA85b] appears as strong arguments against deeply bound $\bar{\text{p}}$-states. A clue to this paradox may be provided by the results of [CL83]. Therein the elastic scattering is calculated using relativistic impulse approximation, i.e., using an average field derived by folding the $\bar{\text{N}}$N t-matrix with the nuclear density. The $\bar{\text{N}}$N potential is simply related to NN potential through *G*-parity (if once again the meson exchange picture holds). Averaging the potential as it is implicitly done if the Dirac phenomenology keeps this *G*-parity structure. However, going from the potential to the t-matrix and folding the t-matrix alters this structure. This point has not been discussed carefully however, to the best of our knowledge.

4.6 Annihilation channels.

4.6.1 *Introduction.* — The annihilation can be studied through the particles which are emitted after this process. Inclusive (charged) pion and proton emission have been carefully measured at LEAR [Mc86]. Negative pion and charged particle multiplicities have been measured with streamer chamber on ^{4}He [BA84a, BA85] and ^{20}Ne [BA86] targets and with emulsion [BA86a]. Some strange particle yields have been studied in the past [CO84], and also on ^{20}Ne target in the LEAR regime [BA87], and for 4.4 GeV/c antiprotons at KEK [MI84]. Neutron spectra have been measured in one case [BÜ88]. Recently, composite (d, t, ...) particle spectrum have been reported [vo88]. Finally, fission yields have been recently measured. (The last three quantities have been obtained at rest only). In section 4.6.4, we will mainly discuss these cross-sections. We postpone the analysis of some of them to section 5, for reasons which will appear later.

4.6.2 *Non strange particles.* — The inclusive pion and proton cross-sections have been measured at LEAR by the PS187 experiment group on two targets : ^{12}C, ^{89}Y, ^{238}U. The results are shown in figure 8. They are well reproduced by the INC calculation of references [Mc86, CL82]. Similar trends are obtained with the Liège code [DE88]. An interesting feature emerges when the quantity $d\sigma/p^2\,dp$ is plotted against the energy E (Fig. 9). Indeed, if the emission is due to a single thermal source, the quantity above appears as an exponentially decreasing line in the plot of figure 9. The slope parameter can then be translated as a temperature. For pions, two *sources* seem to appear. The one with the largest temperature ($T \approx 110$ MeV) obviously corresponds to the primordial pions. The second source ($T \approx 50$ MeV) comes from the rescattering of these pions as is extensively explained below. The protons exhibit a temperature of the order of ≈ 50 MeV. It cannot be stated from the data that there exists a source of smaller temperature. The interpretation of these features is contained in section 4.6.5. When going from ^{12}C to ^{238}U, the pion cross-section increases roughly by a factor 4, whereas the proton cross-section is increased by a factor ~ 15, although the shape of the

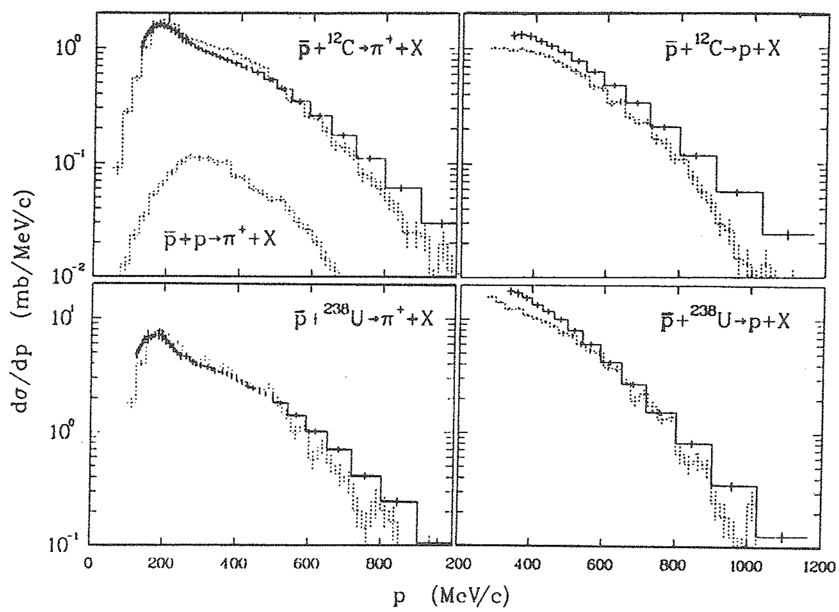

Fig. 8. — The angle-integrated inclusive momentum distributions for π^+ and protons from 608 MeV/c antiproton annihilation on ^{12}C and ^{238}U. The solid histograms are the data and the dashed histograms represent the INC calculations, both from [Mc86]. The second dashed curve in the upper left frame represents the momentum distribution of pions from antiproton-proton annihilation at the same momentum.

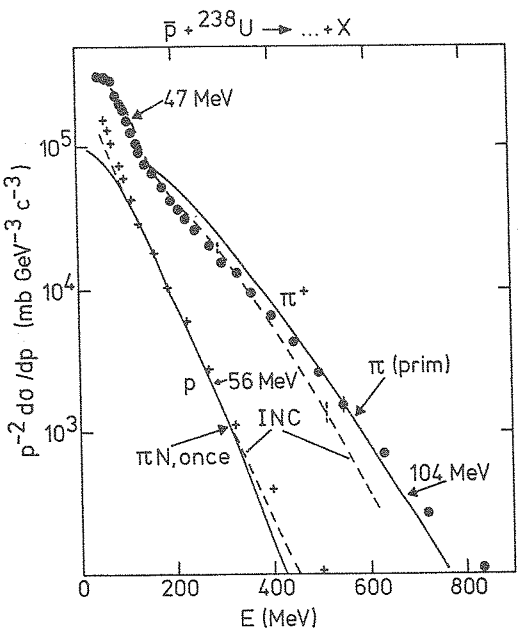

Fig. 9. — Inclusive pion and proton $d\sigma/dp^3$ cross-sections for $\bar{p}$ (608 MeV) + ^{238}U. Dots and crosses : experimental data of [Mc86] ; dashed lines : INC calculations of [CU88]. The full lines give the primordial pion spectrum and the contribution of the nucleons which have been hit once only, respectively. The corresponding temperatures are indicated (see text for detail).

spectrum is not very much changed. The latter factor is slightly higher than the ratio $(A_1/A_2)^{2/3}$, but one needs integrated cross-sections to really draw conclusion from this comparison.

The angular distribution of the emitted particles is also noteworthy. Although the protons are fairly isotropic in the lab system with a small backward peaking, the pions are definitely forward peaked.

Pion and charged particle multiplicity results are provided by the streamer chamber group at LEAR [BA85]. Concerning negative pions, the average multiplicities are contained in table VI. If one takes the values of section 2.3 for π^- abundances in $\bar{N}N$ annihilation, one finds that the ratio of the final π^- abundance to the primordial one $\pi_f^-/\pi_{pr}^- \approx 0.84$, which gives a direct measure of the pion absorption in Ne (at rest). The charged particle multiplicity distributions have been measured for $\bar{p}$-^{4}He, $\bar{p}$-^{20}Ne, $\bar{p}$-emulsion [BA85, BA87, BA86a]. Some results are contained in figure 10. For ^{20}Ne, high multiplicity events correspond to a total desintegration of the target. In emulsion, up to $M \approx 25$ events occur (with a low probability, of course), but they cannot be assigned to desintegration of the heavy targets (Ag/Br). Note, however, that some fraction of the tracks, both in Ne and in emulsion, are due to particles heavier than protons. Their percentage is not known, unfortunately.

TABLE VI. — *Pion multiplicity in $\bar{p}$-nucleus annihilation.*

	p_{lab}	$\langle\pi^+\rangle$	$\langle\pi^-\rangle$	$\langle\pi^+\rangle/\langle\pi^-\rangle$	$\langle\pi^+\rangle_{pr}$	$\langle\pi^-\rangle_{pr}$	$(\langle\pi^+\rangle/\langle\pi^-\rangle)_{pr}$	$P_a^{(+)}$	$P_a^{(-)}$
^{12}C	600	1.01	1.32	0.77	1.29	1.79	0.72	0.22	0.26
^{20}Ne	0 (rest)		1.50		1.29	1.79			0.16
^{20}Ne	600		1.37		1.29	1.79			0.23
^{89}Yt	600	0.78	1.11	0.67	1.26	1.82	0.69	0.38	0.39
^{238}U	600	0.69	1.03	0.66	1.24	1.87	0.66	0.44	0.45

The second and third columns give the observed average multiplicity. The symbol « pr » stands for « primordial ». The quantity $P_a^{(+)}$ and $P_a^{(-)}$ gives the average probability for absorption. See text for detail. The experimental data are taken from [Mc86, BA87, BA88].

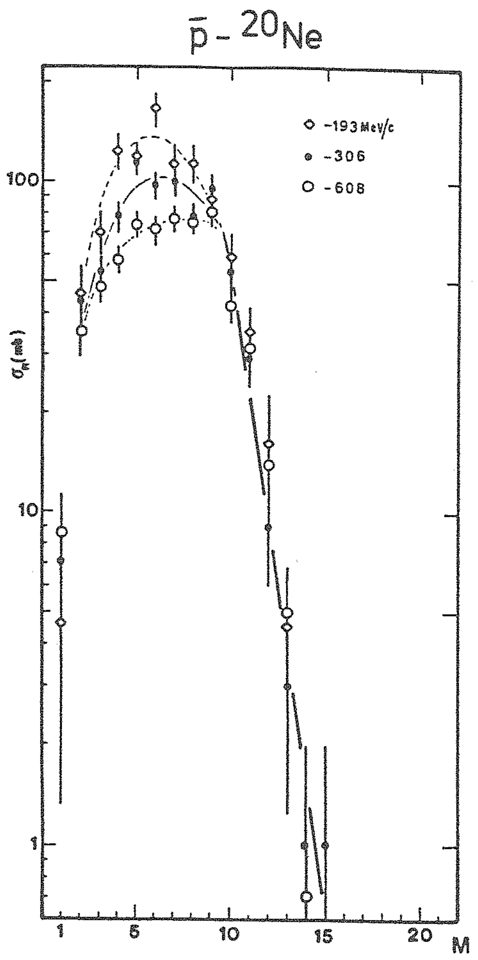

Fig. 10. — Charged particle multiplicity distribution in ^{20}Ne for three values of $\bar{p}$ incident momentum. Adapted from [BA86].

In ^{20}Ne, the authors of reference [BA85] noticed a strong correlation between the average π^- multiplicity and the total charged prong multiplicity M for $M \gtrsim 9$. This puzzling result was explained recently [CU88] as due to the conservation of charge. The argument relies on the fact that the initial charge being equal to 9, any event with $M \geqslant 10$ must contain n negative pions at least, where n is the integer part of $(M-8)/2$.

Composite particle production has been studied recently [vo88, MA88] in annihilations (at rest) on targets ranging from ^{12}C to ^{238}U. Particles from p to ^{8}Be in various kinematical ranges are detected and separated, but ^{3}He and ^{4}He have only been analyzed up to now. The energy spectra dN/dE shows an exponential shape, $\sim e^{-E/E_0}$ with a parameter E_0 which does not vary with the target. When the spectra are parametrized as e^{-p^2/p_0^2}, a single parameter $p_0 \approx 345$ MeV/c fits both the ^{3}He and the ^{4}He spectra. The ^{4}He/^{3}He ratio increases with the target mass. This has been interpreted as resulting from successive pick-ups of protons and neutrons. The universality of the parameters E_0, also encountered in reactions induced by pions [MA88a] or high energy protons [KA85], indicates an origin linked with the end of the production process, when the target has somehow lost the memory of how it has received the excitation energy.

4.6.3 *Strange particle channels.* — Strange particles are created during the annihilation with a small rate (see Sect. 2). In the LEAR regime, the annihilation itself is the only source, since cascading pions are not energetic enough to produce strange particles. But the cascade may modify both the abundance and the spectrum of the strange particles issued from the annihilation.

Except for experiments on deuteron targets, there are very few measurements available. Charged kaons are measured [SM88] in $\bar{p}$-nucleus at rest and $K^\pm/\pi^-$ ratios are extracted for momentum larger than 500 MeV/c. Neutral strange particle yields have been measured through their charged particle decay modes : Λ^0 in $\bar{p}$ (350 MeV/c)-nucleus [CO84], Λ^0, $\bar{\Lambda}^0$, K_S^0 in $\bar{p}$ (4 GeV/c)-Ta [MI84], Λ^0, K_S^0 in $\bar{p}$ (608 MeV/c)-^{20}Ne [BA87]. The results are summarized in table VII. Strange particle production is clearly enhanced while antilambda's are depressed, compared to the $\bar{p}p$ case. In $\bar{p}p$, only $K\bar{K}$ pairs can be produced at low energy. The $\Lambda\bar{\Lambda}$ threshold corresponds to ~ 1.5 GeV/c $\bar{p}$'s. The subsequent cascade can transfer strangeness (through e.g. $K^- N \to \pi\Lambda$) or produce hyperons (through e.g. $\pi N \to K^+ \Lambda$) if the energy is large enough. The cross-sections are of a few mb. A semi-quantitative analysis [KO87] has been performed for the $\bar{p}$-Ta case at 4 GeV/c. It shows that the secondary reactions in the cascade plus the possible transformation of primordial Σ's in Λ^0 could explain the Λ yield. It would be nice to have the K^+ yield (in the LEAR regime), since the latter is practically not altered in the cascade [Di84].

A puzzling aspect of these measurements is the emission pattern for the Λ's and the K_0's in references [MI84, BA87]. They look fairly isotropic in some moving frame. When the velocity of the latter are translated in terms of $\bar{p}+$ (x nucleons) systems, one finds that the Λ source corresponds to $x \approx 12$-13 in both experiments. For the K_S^0, one finds $x \approx 3$ in [MI84] and

TABLE VII. — *Some strange particle yields.*

	K^+/π^-	K^-/π^-	Λ	$\bar{\Lambda}$	K^0_S
$\bar{p}$-H, rest	2.2	2.2			
$\bar{p}$-d, C, U rest	2.8	3.0			
$\bar{p}$-C, Ti, Ta, Pb 350 MeV/c			1.9 ± 0.4		
$\bar{p}$-^{20}Ne 608 MeV/c			1.95 ± 0.43		0.85 ± 0.17
p-Ta 4 GeV/c			11.85 ± 1	0.23 ± 0.1	5.0 ± 0.2
$\bar{p}$-p at rest	1.5	1.5			2.3 ± 1.0
$\bar{p}$-p 4 GeV/c			0.96	0.80	3.4
$\bar{p}$-p 1 GeV/c					3.0 ± 1.0

The origin of the data is given in the text.

$x \approx 1$ in [BA87]. A clear interpretation of these numbers is not existing yet (see however Sect. 5).

4.6.4 *The INC model.* — For in flight annihilations, three groups (at least) have built an INC code [CL82, IL82, CA82, CA83, CU85, CU87, JA88], which seem very close to each other in their spirit and in their predictions. Roughly speaking, they are based on three assumptions : (1) the antiproton annihilates on a nucleon, chosen according to its motion in the potential created by the target and to the $\bar{N}N$ annihilation cross-section (see Sect. 2.1). The annihilation releases a certain number of pions, which is chosen according to equations (2.10)-(2.11). The charge of these pions is usually taken from a statistical model reproducing the mean experimental values [GH74], whereas their momenta are generated according to the phase space density. This is known to generate a thermal-like spectrum in the annihilation frame, with a temperature in the neighbourhood of 110 MeV ; (2) the pions start cascading through the nucleus, possibly ejecting nucleons when colliding with them. This part is exactly the same as for annihilation at rest (Sect. 3.4.2) ; (3) after some time (which depends upon the incident energy and upon the target but which is typically ~ 30-50 fm/c), the cascade is turned off. The rest of the dynamical process is described by an evaporation model, as for annihilation at rest [IL82, JA88].

The INC model revealed itself quite successfull in describing the inclusive proton and pion cross-sections [Mc86, CA83, CU85, DE88], the neutron spectrum [CU88], the pion multiplicities [CU85, IL82], the mass spectrum of the residues [IL82, CU88]. The accuracy is sometimes very good, but may be sometimes ~ 20-25 % off (see high energy pions in Ref. [Mc86]). This is quite reasonable in view of the fact that the model has no free parameter. Of course, it can miss some physics, like the medium corrections to pion propagation, which has recently drawn the attention, mainly in the heavy ion context [GA87, LE88], but also for the annihilation [HE86]. It is not sure that the discrepancy can be attributed to these effects.

4.6.5 *INC dynamics.* — One of the striking feature of figure 9 is the existence of Maxwell-Boltzmann-like tails in π^+ and p spectra with large corresponding temperature. This should not be interpreted as the evidence of considerable heating of a piece of nuclear matter. The high energy tail of the π^+ spectrum comes from the tail of the spectrum of the primordial pions, which is thermal-like, as we explained in section 2. Thus this part of the spectrum is due to *non-interacting* pions. The high energy tail of the proton spectrum is due to a single hit by high energy pions as it is demonstrated in figure 9 where one has recorded in an INC calculation [CU88] the contribution of the protons which have made one collision with a pion only. The Maxwell-Boltzmann tail of the primordial pion spectrum is reflected in the Maxwell-Boltzmann tail of the proton spectrum.

Rather than giving rise to a thermal source, the INC dynamics is in fact closer to *multi-spallation*. The interacting pions whose number is between 2 and 3 (due to the peripheral nature of the annihilation in the LEAR regime) travel through the nucleus ejecting a nucleon from time to time. Actually, they made only ~ 3-4 collisions [CU87, Mc86b]. These collisions are rather hard, however, and the transfer of energy from the multipion system to the baryon system is nevertheless efficient. The energy transfer is of the order of 600 MeV on the average for the case shown in figure 11, but may fluctuate largely around this value. However, this energy is quickly carried away from the nucleus by high energy protons and the excitation left as random excitation of the target is rather small, typically between 100 and 200 MeV as indicated by figure 12. As we already mentioned,

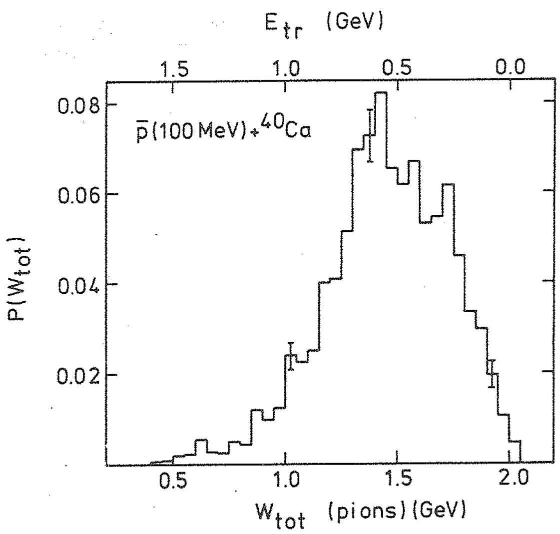

Fig. 11. — Distribution of the energy transfer E_{tr} (upper scale) and of the final pion energy (lower scale) in $\bar{p}$ (100 MeV) + ^{40}Ca.

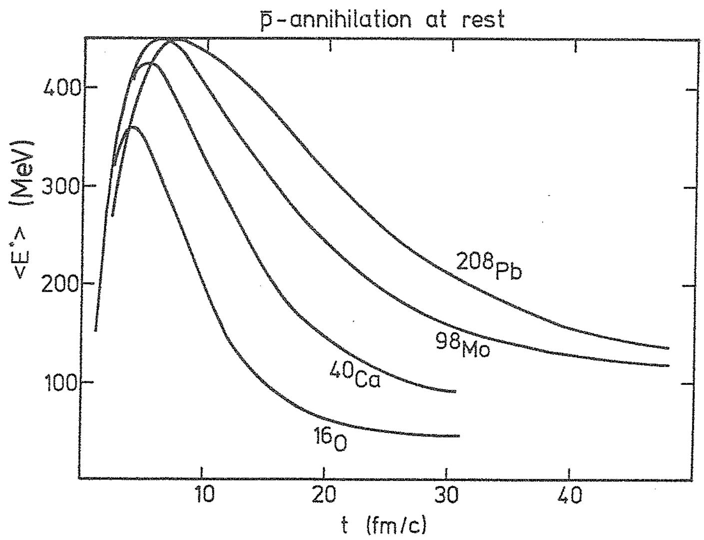

Fig. 12. — Time evolution of the excitation energy contained in the target volume (adapted from [CU87a]).

the excitation energy is thereafter released by evaporation. We have seen that in the $\bar{p}$-annihilation at rest, the distribution of the residue is consistent with this energy transfer.

The production (in the sense of ejection) of particles through independent *sub-processes*, like the pion cascades, can leave a signature in the total (and some partial) charged particle multiplicity distribution, according to [GI86a]. The latter takes the form of a negative binomial, a mathematical function with two parameters. One is the number of sub-processes, named « clans » and the other is the average of number particles inside a clan. The experimental charged particle distributions available are well reproduced by negative binomial [CU87b]. However, the analysis gives a number of clans larger than the number of primordial pions, which is not very satisfactory from the physical point of view. We note, however, that recently, a dynamical clan model has been built with a number of clans closer to the known number of interacting pions. The model does not lead exactly to a negative binomial, but is very consistent with experimental data [CU88a].

4.6.6 *Interest for nuclear physics.* — The $\bar{p}$-annihilation on a nucleus allows for the study of the interaction of a nucleus with a multipion system or, more generally with a multi-meson system. Although the interest of such a process is accepted by everybody, precise questions have not been addressed yet. For conventional nuclear physics, the annihilation presents some interest, which has been raised in [CU86]. A currently open problem is the way an excited nucleus loses its binding. The commonly accepted ideas are the following. If the excitation energy is under some specific value E_c^*, the nucleus keeps its cohesion, losing a few nucleons by evaporation. If this excitation energy is larger, the nucleus loses its cohesion, and fragments in many pieces of intermediate size ; this is the so-called multifragmentation. Specific questions are : (1) what is the value of E_c^* ? ; (2) is the transition rapid ? ; (3) does the mode of energy injection matter ? Such questions are intensively studied with heavy ions and are beginning to receive at least partial answers. For instance, it is believed that $E_c^* \approx$ 3 MeV [DE87]. It would nevertheless be useful to study these questions with antiprotons. The latter present the advantage that the reaction dynamics is better understood, and that the energy transfer is not very sensitive to the impact parameter. Furthermore, one can vary the energy deposit by changing the $\bar{p}$ energy. The LEAR domain seems to be in the subcritical regime, at least for heavy targets [CU86], but 1 GeV antiprotons should provide overcritical conditions.

4.6.7 *Hot hadronic spots.* — It is important to know what is the energy of the nucleus after the pion cascade, because it is then more or less randomized on the whole nucleus. Another as important point is the energy transfer from the multipion system to the nuclear system. If this transfer is quicker and a little more evenly distributed than in the INC picture one may expect to have realized a small piece of hadronic matter (with $B \approx$ a few units) with high excitation energy. Of course, as in the INC, a large part of this energy should be removed by high energy spallation nucleons, because the measured residue distribution is certainly more consistent with a randomized nucleus excitation of 100-200 MeV rather than 600 MeV.

It is then interesting to try to determine the energy transfer E_{tr}. The available experimental data are not suited for this purpose. The success of the INC for reproducing the pion spectra gives some confidence in the INC estimate of E_{tr}. But the question can be solved by experiments dedicated to this purpose. They require charged particle detectors and a neutron calorimeter. This technique is certainly available nowadays.

5. Special topics.

5.1 HYPERNUCLEUS FORMATION. — In a series of beautiful measurements [BO86, BO87, EP85, EP86], Polikanov and his collaborators have studied the possibility of making hypernuclei through $\bar{p}$ annihilation on nuclei. The method relies on the study of the fission decay in $\bar{p}$-U or $\bar{p}$-Bi experiments. Delayed fission is observed and is separated from the prompt one, using the so-called recoil-distance method which was developed to study fission isomers. The recoiling nucleus gets out of the target and travels for some distance before decaying. The fission fragments are then collected downward in a position sensitive detector. The delayed fission lifetime is about $(2 \pm 1) \times 10^{-10}$ s and $(1.5 \pm 0.6) \times 10^{-10}$ s for Bi and U, respectively. This large values strongly suggest that the delayed fission results from the formation of an hypernucleus and the subsequent non mesonic (collision) decay of the hyperon

$$\Lambda + \mathrm{N} \rightarrow \mathrm{N} + \mathrm{N} . \tag{5.1}$$

This process releases ~ 170 MeV which is sufficient to trigger the fission process.

This new experiment has renewed the interest for hypernucleus physics. Indeed, only lifetimes for light hypernuclei were known before. Specific questions are dealing with the detail of the strangeness changing weak interaction responsible for process (5.1) and the importance of short-range correlations for its probability.

The formation of hypernuclei through p̄-annihilation presents some interest connected with the dynamics of the annihilation as will be described in the next section.

5.2 ANNIHILATION ON TWO NUCLEONS. — The simplest picture, largely dominated by Dirac's concept of charge conjugation, says that an antiproton annihilates on a nucleon in a very localized region of space giving rise to asymptotically free pions (except for resonances, as we said in Sect. 2). However, very early after the discovery of the antiproton, Pontecorvo [PO56] drew attention to the possibility of having unusual final states if the annihilating nucleon is bound in a nucleus. Indeed, another nucleon may be involved in the process before the pions are asymptotic. The simplest example which illustrates this statement is the p̄d system. The annihilation may occur on a single nucleon, say the proton, and the neutron remains a spectator. Therefore the lowest pion multiplicity is reached in reactions

$$\bar{\mathrm{p}}d \rightarrow \begin{cases} \pi^+ \, \pi^- \, \mathrm{n} \\ \pi^0 \, \pi^0 \, \mathrm{n} \end{cases} . \tag{5.2}$$

On the contrary, if the neutron is directly involved in the process, the following reactions become possible

$$\bar{\mathrm{p}}d \rightarrow \begin{cases} \pi^- \, \mathrm{p} \\ \pi^0 \, \mathrm{n} \end{cases} . \tag{5.3}$$

Note also the following possibilities

$$\bar{\mathrm{p}}d \rightarrow \mathrm{K}^- \, \Sigma^+ \tag{5.4a}$$
$$\bar{\mathrm{p}}d \rightarrow \bar{\mathrm{K}}^0 \, \Lambda^0 . \tag{5.4b}$$

In the annihilation involving three nucleons, one may have no-meson process, like

$$\bar{\mathrm{p}} + {}^3\mathrm{He} \rightarrow \mathrm{p} + \mathrm{n} \tag{5.5a}$$

or

$$\bar{\mathrm{n}} + {}^3\mathrm{He} \rightarrow \mathrm{p} + \mathrm{p} . \tag{5.5b}$$

Hereafter, we will refer to $B = 0$, 1 or 2 annihilations, if they involve 1, 2 or 3 nucleons, respectively.

Historically, the first experimental indication for $B > 0$ annihilations has been obtained in [BI69], where the process $\bar{\mathrm{p}}d \rightarrow \pi^- \, \mathrm{p}$ is clearly identified by the two-body kinematics. The branching ratio is of course very small (see below ; recently, this branching ratio has been remeasured with a spectrometer by [SM88]). Later on, the momentum spectrum of the proton issued from the process

$$\bar{\mathrm{p}}d \rightarrow \mathrm{K}^0 \, \mathrm{K}^- \, \mathrm{p} + X \tag{5.6}$$

was measured by [OH73]. The spectrum (Fig. 13) shows an important peak at low momentum, which corresponds to the spectator proton (the average momentum inside the deuteron is ~ 100 MeV/c). In addition, there is a long tail, which extends very far in the high momentum domain. The latter cannot be explained by the proton rescattering on K or π^0 meson. It thus corresponds to a large extent to the annihilation on two nucleons. This interpretation was put forward by Rafelski [RA84]. The possibility of having unusual channels after $B = 1$ annihilations was also emphasized by Kahana [KA84].

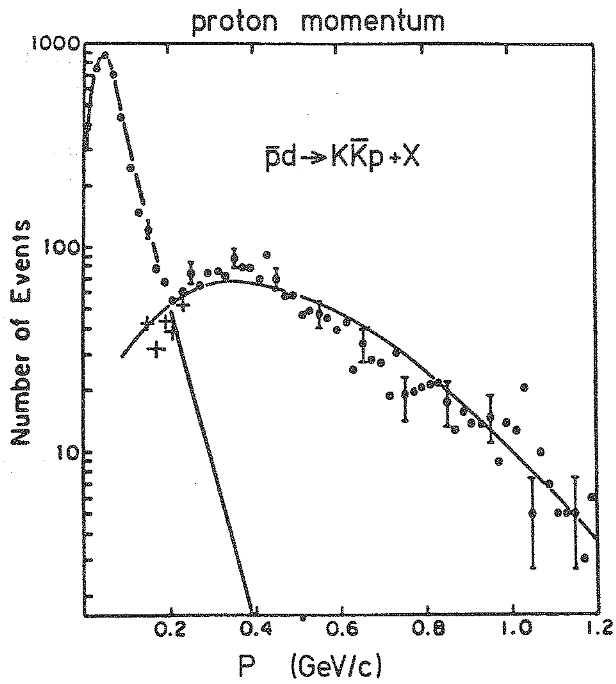

Fig. 13. — Momentum distribution for the outgoing proton in the $\bar{p}d \to K\bar{K}p + X$ reaction. Adapted from [OH73].

A little bit later, it was suggested [CU84a] that $B = 1$ annihilations might be not so unfrequent in nuclei and that they may leave a rather unambiguous signature. The first statement is based on the following simple consideration. Any hadronic interaction like $\bar{p}N$ annihilation takes some time (of the order of 1 fm/c, since hadron sizes are of the order of 1 fm). Therefore the $\bar{p}N$ system travels for some distance inside the nucleus before decaying. In the meantime, it thus has some chance for interacting with another nucleon. This probability is directly linked with the lifetime τ of the $\bar{p}N$ *intermediate* state (fireball in the terminology of [HA78]), which is not known precisely. If $\tau = 1$ fm/c, the probability can be as high as 30 % in the LEAR regime. (It should be larger at larger energy).

The properties of the $B = 1$ as well as $B = 0$ and $B = 2$ annihilations have been studied [CU84], using the simplest assumption, namely that the decay of the annihilating system is governed by phase space. In other words, the decay is described in the frame of a microcanonical ensemble calculation. The rate for a given multiplicity n is given by

$$f(\sqrt{s}\,; m_1, \ldots, m_n) = C_0^{n-2} R_n(\sqrt{s}\,; m_1, \ldots, m_n)\,, \tag{5.7}$$

for non-strange channels and

$$f(\sqrt{s}\,; m_{\mathrm{K}}, m_{\bar{\mathrm{K}}}, m_1, \ldots, m_\ell) = \beta C_k^\ell R_{\ell+2}(\sqrt{s}\,; m_{\mathrm{K}}, m_{\bar{\mathrm{K}}}, m_1, \ldots, m_\ell) \tag{5.8}$$

where R_n is the invariant phase space integral [HA63], the m_i's are the masses of the produced particles and $\sqrt{s}$ is the c.m. available energy. There are basically two free parameters, namely C_k/C_0 and β, but β is introduced to reproduce finer details (like the distribution of the pion multiplicity in strangeness producing annihilations). These two parameters are fitted on $B = 0$ annihilation properties. The model can then make predictions on the branching ratios for various final channels. The most important of these predictions is the significant enhancement of strange particle production in $B = 1$ annihilations, compared to $B = 0$. This is a direct consequence of phase space since for instance the ΛK channel in $B = 1$ annihilation lies well below the K$\bar{\mathrm{K}}$ channel in $B = 0$. This conclusion is illustrated in table VIII, which reproduces some branching ratios.

Some existing data on strangeness production have been analyzed [CU88] in the light of these considerations. We just give the main results of this analysis.

(a) $\bar{p} + d$. This system has been studied in [BI69] for the $\bar{\mathrm{p}}d \to \mathrm{p} + \pi^-$ channel, in [OH73] for the $\bar{\mathrm{p}}d \to \bar{\mathrm{K}}\mathrm{Kp}$ channel and recently by [SM88]. The very observation of the exclusive pπ^- channel [BI69] is already an evidence for $B = 1$ annihilation. In the $\bar{\mathrm{p}}d \to \bar{\mathrm{K}}\mathrm{Kp}$ reaction, the protons are observed with a very high momentum tail, totally unconsistent with a *spectator* proton, which would have only the average momentum inside the deuteron. The importance of this tail indicates that $B = 1$ annihilations occur about 10 % of the time. With this frequency and using reference [CU84a], one can make definite predictions for the branching ratios for $\bar{\mathrm{p}}d \to \mathrm{p}\pi^-$ and $\bar{\mathrm{p}}d \to \Lambda + X$: they turn out to be 4.7×10^{-5} and 7.6×10^{-3} respectively. They compare rather well with experiment, which yields 2.8×10^{-5} and 3.6×10^{-3} respectively.

(b) $\bar{p}$-nucleus. The theoretical problem here is to determine the frequency of $B = 1$ annihilations. Only crude estimates are made in [CU84a], based on geometrical considerations only. Anyway, we can look whether pure $B = 0$ annihilations are sufficient to reproduce some observables involving strangeness. The latter can be :

(1) K^+ yield : the K^+ abundance is practically unchanged by the cascade process since K^+ scatters only elastically with the nucleons. At rest, the K^+ abundance in $\bar{\mathrm{p}}$p is 0.025 per annihilation. An enhancement in $\bar{\mathrm{p}}$ nucleus would indicate the presence of $B = 1$ annihilation. Unfortunately, there is no measurement available up to now.

(2) K^+/π^- ratio : this ratio may be easier to measure since it does not require a measurement over a large angular range. However, the situation is a little bit complicated here since pions can be absorbed and since large nuclei (N > Z)

TABLE VIII. — *Branching ratios (in %).*

	π's only	$\langle n_\pi \rangle$	$\bar{K}K$	ΛK	ΣK	$\langle K^+ \rangle$	$\langle K^+/\pi \rangle$	$3\,\bar{s}/\bar{q}$
$\bar{p}p$, at rest	95	5.01	5			~ 2.5	0.5	
$\bar{p}p$, microcan. [CU84a]	95.5	5.05	4.5					
$\bar{p}NN$, microcan. [CU84a]	88.5	4.73	2.71	2.86	5.52	5.5	1.4	11
$\bar{p}(3N)$, microcan. [CU84a]	85.4	4.36	1.77	4.32	8.07		0.019	
quark-gluon $T = 200$ MeV							25	
quark-gluon, $\bar{p}p$ [PH85]		4.5					0.5 if $F = 0.1$	
$\bar{p}A$, cannon. [DE85]								10-15

favour π^-'s. This should perhaps explain the observations of [SM88]. The last problem can be minimized by using $N = Z$ nuclei and/or considering the $K^+/(\pi^- + \pi^+)$ ratio.

(3) Λ^0 production : this has been measured by [CO84] with a poor statistics. On the average, they observe $\sim (1.9 \pm 0.4) \times 10^{-2}$ Λ^0 per annihilation. This figure could be obtained with $B = 0$ annihilations only if all the $\bar{K}$'s transform into Λ by scattering through the nucleus. This obviously is not plausible in view of the small $\bar{K}N \to \Lambda\pi$ cross-section (see below).

(4) Hypernuclei formation : this refers to the delayed fissions discussed in section 5.1. The mechanisms which produce the hypernucleus can be either (a) $\bar{p}N \to K\bar{K}$, $\bar{K}N \to \Lambda\pi^-$, followed by the fixation of the hyperon on the nucleus, or (b) $\bar{p}NN \to \Lambda K$, followed by the fixation of the Λ. The first mechanism is plausible, since the $\bar{K}$ issued from the annihilation has just the momentum (~ 700 MeV/c), which favours the substitutional fixation of the Λ created by $\bar{K}N \to \Lambda\pi^-$ [PO76]. Let P_0 and P_1 be the relative probability of the $B = 0$ and $B = 1$ annihilations, P_r the probability for a $\bar{K}$ to make a $\bar{K}N \to \Lambda\pi^-$ reaction inside the nucleus, and $P_f^{(0)}$, $P_f^{(1)}$ the fixation probability of the Λ in $B = 0$ and $B = 1$ cases. The yield of hypernuclei per annihilation is then given by

$$Y = P_0\, B_{\bar{K}}^{(0)}\, P_r\, P_f^{(0)} + P_1\, B_\Lambda^{(1)}\, P_f^{(1)}, \tag{5.9}$$

where $B_{\bar{K}}^{(0)}$ and $B_\Lambda^{(1)}$ are the branching ratios for $\bar{K}$ production in $B = 0$ and Λ production in $B = 1$ respectively. Assuming $P_0 = P_f^{(0)} = 1$, $B_{\bar{K}}^{(0)} = 0.06$, and evaluating P_r with $\sigma(\bar{K}N \to \Lambda\pi^-) = 1.6$ mb, one obtains $Y = 10^{-4}$ at the most [EP86]. The observed yields are 3×10^{-4} and 9×10^{-4} for Bi and U respectively.

The latter can be explained only if the $B = 1$ annihilations are possible. With $P_1 \approx 0.1$, the experimental value is obtained, if $P_f^{(1)} \approx 10^{-1}$ for Bi, which seems quite reasonable.

5.3 QUARK-GLUON BLOBS. — The possibility that $\bar{p}$-annihilation could lead to the formation of a quark-gluon plasma inside the nucleus was first proposed by Rafelski [RA80]. However, it is not expected that the whole nucleus will be transformed into quark-gluon plasma. This would require a tremendous excitation, since it is believed that quark-gluon formation needs energy density ~ 2 GeV fm^{-3}. Therefore, the name of quark-gluon blob has been coined, which means a system with freely moving quarks in a volume of limited dimension. A possible consequence of the blob could be an enhancement of strange particle formation. The argument, first announced for the case of the heavy ion collisions [RA82], is that strangeness creation is much easier in the plasma phase compared to the hadronic phase. Strangeness will always be saturated in a plasma of a lifetime larger than ~ 5 fm/c. According to the authors of [RA82], the strange quarks will be quite numerous, if the temperature is above the critical temperature ($T_c \approx 180$-250 MeV). Therefore the best signature in that respect is the abundances of particles with several quarks : Ξ, Ω or even better $\bar{\Xi}$, $\bar{\Omega}$.

This idea has been applied to $\bar{p}$-annihilation. In [PH85], the $\bar{p}p$ system itself was considered as a quark-gluon blob. It is assumed to be at equilibrium, but, in order to get good agreement with experiment, the s-quark degrees of freedom should be saturated to 10 % only. This is indicated in table VIII.

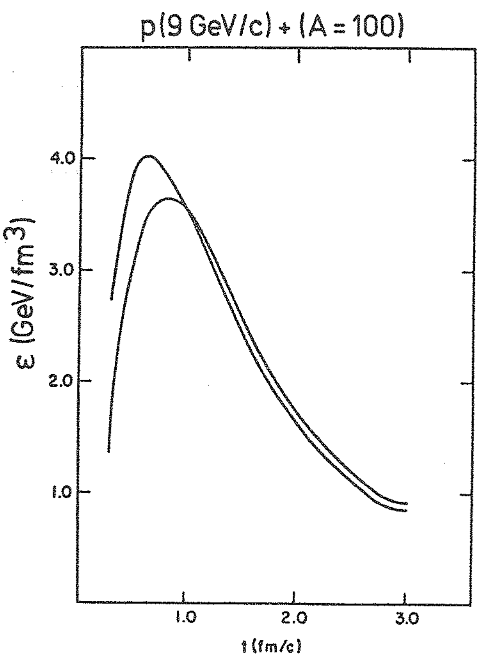

Fig. 14. — Energy density ε as a function of time in the fireball produced by the $\bar{p}$ (9 GeV/c) + ($A = 100$) central collisions, as calculated by [GI86].

Up to now one has to admit that there is no real indication of formation of quark-gluon plasma. Recently, Rafelski [RA88] analyzed the Λ and K_S^0 yield in $\bar{p}$ (4 GeV/c) + Ta reaction [MI84]. Assuming a fireball is formed with antiproton and a few nucleons, he extracts the temperature, the energy per baryon, and possibly the entropy. These conditions can be those of a (baryon rich) plasma, but a chemical potential of 395 MeV is required, which corresponds to baryon density $\approx 2.5\,\rho_0$. This compression is in strong contradiction with INC calculations [CA82, CU87a], and even with hydrodynamical calculation [ST82]. Note that the $\bar{p}$-Ta data have not been studied with the ideas of section 5.2.

Another, more conventional, mechanism for quark-gluon plasma formation with antiprotons has been studied in [GI86, ST84]. Annihilation of high energy antiprotons (~ a few GeV) even on a single nucleon can produce high energy density since the multipion system travelling forwardly and with high speed can sweep a large piece of matter in front of it. This is illustrated in figure 14.

5.4 DISCUSSION. — The annihilation on two nucleons introduces new ideas about the dynamics of the annihilation. The model of [CU84a] being a phase space model does not introduce a detailed dynamics (this is illustrated by a box in Fig. 15(d)), but nevertheless implies strong interaction between the two nucleons.

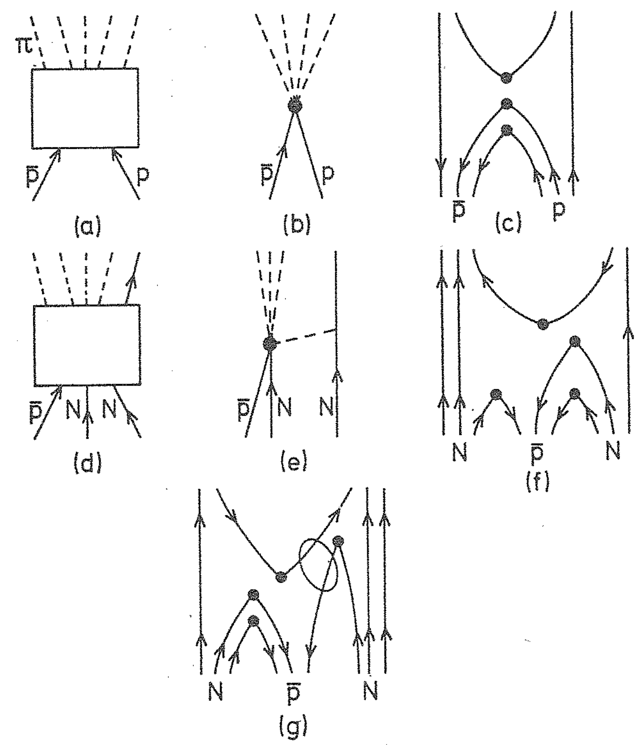

Fig. 15. — Schematic diagrams for $B = 1$ annihilation in a phase space model (d) [CU84a], in a mesonic model (e) [OS88] and in a quark model (f). The corresponding diagrams for the $B = 0$ annihilation are given by the first row. The meaning of graph (g) is explained in the text.

Translated into mesonic degrees of freedom, this can be represented (at the simplest level) by graph 15(e), where a pion created off-shell is absorbed by the second nucleon (on put on-shell by scattering on it) [OS88]. In terms of quark degrees of freedom, the annihilation on two nucleons can be viewed as in figure 15(f). (Here for simplicity, the quark diagrams are drawn for simple final state only). Note that graphs (c) and (f) are not so different since only one additional $q\bar{q}$ annihilation occurs in graph (f). The annihilation on two nucleons however allows $q\bar{q}$ annihilations which are not grouped according to $\bar{p}p$ conjugation. Indeed a $\bar{q}$ of the antiproton annihilates with a quark of the first nucleon, whereas the other $\bar{q}$'s annihilate with the quark of the second nucleon. This observation calls for two consequences :

(1) If antiquarks are introduced in a nuclear medium (under the form of an antibaryon), their evolution is not necessary dictated by charge conjugation at the global (bag) level. The pure charge conjugation (in the Dirac sense) appears at the quark level.

(2) The antiquarks in this process can be considered as being partially delocalized, since they reach two neighbouring bags. Of course, this can occur if the two nucleons are close enough to the antiproton. Therefore, this delocalization should be limited. If qualitatively this ressembles to the expected properties of a quark-gluon blob, the latter should be characterized, we think, by a longer *delocalization length.* One can also consider that the meson graph (e) implies the notion of delocalization. Indeed, graph (g), topologically similar to graph (f), is the quark counterpart of graph (e), where the intermediate $q\bar{q}$ pair (encircled) plays the same role as the meson in graph (c).

One may thus wander whether all these models (phase space, meson exchange, quark diagrams, quark-gluon blobs) do share the same physics, namely, partial delocalization. This would certainly desserve further investigation.

6. Outlook. Conclusion.

The antiproton-nucleus interaction is largely dominated by strong annihilation. This probe is thus not very appropriate to study the inner shells of the nucleus, nor fine spectroscopic details (except for charge exchange and some inelastic scattering).

The strong $\bar{p}$-annihilation on nuclei presents nevertheless important interest from three points of view, each of which has not been intensively studied up to now :

(1) It is a complementary way to deposit energy inside a nucleus. It presents some advantages compared to conventional beams (heavy ions, high energy protons, ...) and is a suitable mean to study multifragmentation, its properties and the onset of this phenomenon.

(2) It can shed some light on the annihilation process and extends our understanding of the charge conjugation concept. In particular, the study of the two nucleon annihilation should be pursued. Strangeness yield measurements are a good way to look at it, but other signals should be searched for. More generally,

signals for unusual annihilations have to be studied. The simplest of which can be the multiplicity of some particles. These studies could in principle tell us whether annihilations (even on one nucleon) are altered because of the presence of the nuclear medium.

(3) It may open a branch of hadronic physics not studied up to now. We think to a multimeson system in a baryon rich medium. This may give rise to new states of hadronic matter. Without resorting to this exceptional though fascinating prospect, one may also use $\bar{p}$-nucleus annihilation to study a whole set of exotic nuclei containing various particles (not easily formed otherwise) or baryonic or mesonic resonances. The experiments on hypernuclei are already a good illustration of this point. One may also think to η-nucleus, since annihilation is a good source of η's, but also to ω- nucleus. This program (as well as program (1)) will certainly benefit from using $\bar{p}$'s more energetic than those of LEAR, in the GeV range for instance.

We want to thank P. Deneye and M. Jaminon for useful discussions.

References

[AD87] Adachi S. and von Geramb, H. V., *Nucl. Phys.* **A 470** (1987) 461.
[AI81] Aihara, H. *et al.*, *Nucl. Phys.* **A 360** (1981) 291.
[AM87] Amsler, C., *Adv. Nucl. Phys.* **18** (1987) 183.
[AM88] Amsler, C. *et al.* (Eds.) : « Physics at LEAR with Low Energy Antiprotons ». Harwood Acad. Publ., Chur, 1988.
[AR80] Armenteros, R. *et al.*, CERN/PSCC/80-101 (1980).
[AR87] Armstrong, T. *et al.*, *Phys. Rev.* **D 36** (1987) 659.
[AS84] Ashford, V. *et al.*, *Phys. Rev.* **C 30** (1984) 1080.
[AS85] Ashford, V. *et al.*, *Phys. Rev.* **C 31** (1985) 663.
[AU86] Auerbach, N. *et al.*, *Phys. Lett.* **182B** (1986) 221.
[BA64] Barnes, V. *et al.*, Proc. Int. Conf. on High Energy Physics, Dubna (1964) 731.
[BA66] Baltay, C. *et al.*, *Phys. Rev.* **145** (1966) 1103.
[BA84] Batty, C. J., Friedman, E. and Lichtenstadt, J., *Phys. Lett.* **142B** (1984) 241.
[BA84a] Balestra, F. *et al.*, *Phys. Lett.* **149B** (1984) 69.
[BA85] Balestra, F. *et al.*, *Phys. Lett.* **165B** (1985) 265.
[BA86] Balestra, F. *et al.*, *Nucl. Phys.* **A 452** (1986) 573.
[BA86a] Batusov, Y. A. *et al.*, *Europhys. Lett.* **2** (1986) 115.
[BA86b] Batty, C. J., Friedman, E. and Lichtenstadt, J., *Nucl. Phys.* **A 436** (1985) 621.
[BA87] Balestra, F. *et al.*, *Phys. Lett.* **194B** (1987) 192.
[BA88] Balestra, F. *et al.*, private communication.
[BE67] Bettini, A. *et al.*, *Il Nuovo Cim.* **47** (1967) 647.
[BI69] Bizarri, R. *et al.*, *Lett. Nuovo Cim.* **2** (1969) 431.
[BI85] Birsa, R. *et al.*, *Phys. Lett.* **155B** (1982) 397.
[BO82] Bouyssy, A. and Marcos, S., *Phys. Lett.* **114B** (1982) 397.
[BO86] Bocquet, J. P. *et al.*, *Phys. Lett.* **182B** (1986) 146.
[BO87] Bocquet, J. P. *et al.*, *Phys. Lett.* **192B** (1987) 312.
[BR68] Bryan, R. A. and Philipps, R., *Nucl. Phys.* **B 5** (1968) 201.
[BR85] Bradamente, F. *et al.*, Third LEAR Workshop « Physics with Antiprotons at LEAR in the Acol Era » — Tignes 1985. Eds. : U. Gastaldi *et al.*, Editions Frontières, Gif-sur-Yvette, 1985.

[BR86] BRUGE, G., *et al.*, *Phys. Lett.* **169B** (1986) 14.
[BR86a] BRESSANI, T. *et al.*, *Europhys. Lett.* **2** (1986) 587.
[BÜ88] BÜCHE, G., LEWIS, R. A. and SMITH, G. A., in « Physics at LEAR with Low Energy Antiprotons », ed. by C. Amsler *et al.*, Harwood Acad. Publ., Chur (1988), 689.
[CA82] CAHAY, M., CUGNON, J., JASSELETTE, P. and VANDERMEULEN, J., *Phys. Lett.* **115B** (1982) 7.
[CA83] CAHAY, M., CUGNON, J. and VANDERMEULEN, J., *Nucl. Phys.* **A 393** (1983) 237.
[CH88] CHIBA, M. *et al.*, « Physics at LEAR with Low Energy Antiprotons », ed. by C. Amsler *et al.*, Harwood Acad. Publ., Chur (1988) 401.
[CL82] CLOVER, M. R., DE VRIES, R. M., DI GIACOMO, N. J. and YARIV, Y., *Phys. Rev.* **C 26** (1982) 2138.
[CL83] CLARCK, B. C. *et al.*, *Phys. Rev. Lett.* **50** (1983) 1644.
[CO82] CÔTÉ, J. *et al.*, *Phys. Rev. Lett.* **48** (1982) 1319.
[CO84] CONDO, G. T. *et al.*, *Phys. Rev.* **C 29** (1984) 1531.
[CU84] CUGNON, J. and VANDERMEULEN, J., Proceedings of the Winter College on Fundamental Nuclear Physics, eds. : K. Dietrich *et al.*, World Scientific, Singapore (1984).
[CU84a] CUGNON, J. and VANDERMEULEN, J., *Phys. Lett.* **146B** (1984) 16.
[CU85] CUGNON, J. and VANDERMEULEN, J., *Nucl. Phys.* **A 445** (1985) 717.
[CU86] CUGNON, J. and VANDERMEULEN, J., in « Antiproton 86 », ed. by S. Charalambous *et al.*, World Scientific, Singapore (1986) 365.
[CU87] CUGNON, J. and VANDERMEULEN, J., *Phys. Rev.* **C 36** (1987) 2726.
[CU87a] CUGNON, J., JASSELETTE, P. and VANDERMEULEN, J., *Nucl. Phys.* **A 470** (1987) 558.
[CU87b] CUGNON, J., JASSELETTE, P. and VANDERMEULEN, J., *Europhys. Lett.* **4** (1987) 535.
[CU88] CUGNON, J. in « The Elementary Structure of Matter », ed. by J. M. Richard *et al.*, Springer-Verlag, Berlin (1988) 211.
[CU88a] CUGNON, J., DENEYE, P. and VANDERMEULEN, J., to be published (1988).
[DA84] DALKAROV, O. D., SHAPIRO, I. S. and TYAPAEV, R. T., *JETP Lett.* **19** (1984) 46.
[DA85] DALKAROV, O. D. and KARMONOV, V. A., *Nucl. Phys.* **A 445** (1985) 579.
[DA88] DALKAROV, O. D. and KARMANOV, V. A., in « Physics at LEAR with Low Energy Antiprotons », ed. by C. Amsler *et al.*, Harwoord Acad. Publ., Chur (1988) 679.
[DE74] DELOFF, A. and LAW, J., *Phys. Rev.* **C 10** (1974) 2657.
[DE78] DELVILLE, A., JASSELETTE, P. and VANDERMEULEN, J., *Am. J. Phys.* **46** (1978) 907.
[DE85] DERRETH, C. *et al.*, *Phys Rev.* **C 31** (1985) 1360.
[DE87] DESBOIS, J. *et al.*, *Z. Phys.* **A 328** (1987) 101.
[DE88] DENEYE, P., CUGNON, J. and VANDERMEULEN, J., to be published (1988).
[Di84] Di GIACOMO, N. J. and CLOVER, M. R., *J. Phys.* **G 10** (1984) L119.
[DO80] DOVER, C. B. and RICHARD, J. M., *Phys. Rev.* **C 21** (1980) 1466.
[DO83] DOVER, C. B., SAINIO, M. E. and WALKER, G. E., *Phys. Rev.* **C 28** (1983) 2368.
[DO85] DOVER, C. B. and MILLENER, M. E., in « Anticucleon- and Nucleon-Nucleus Interactions, ed. by G. E. Walker *et al.*, Plenum Publ., New York (1985).
[DO86] DOVER, C. B., « Interactions Between Particle and Nuclear Physics ». Lake Louise Conference, ed. by D. F. Geesaman, AIP (1986) 272.
[DO87] DOVER, C. B., IV LEAR Workshop (1987).
[DU56] DUERR, H. P. and TELLER, E., *Phys. Rev.* **101** (1956) 494.
[DU85] DUMBRAJS, O., Third LEAR Workshop « Physics with Antiprotons at LEAR in the Acol Era » — Tignes 1985, ed. by U. Gastaldi *et al.*, Editions Frontières, Gif-sur-Yvette (1985).

[EP85] EPHERRE-REY, CAMPAGNOLLE, M., Third LEAR Workshop « Physics with Antiprotons at LEAR in the Acol Era » — Tignes 1985, ed. by U. Gastaldi *et al.*, Editions Frontières, Gif-sur-Yvette (1985).
[EP86] EPHERRE-REY, CAMPAGNOLLE, M., Proc. INS International Symposium on Hypernuclear Physics. Tokyo (1986) 146.
[FL84] FLAMINIO, V. *et al.*, Compilation of Cross-Section III : p and $\bar{p}$ Induced Reactions. CERN-HERA 84-01.
[FU84] FURAI, S., FAESSLER, A. and KHADKIKAR, S. B., *Nucl. Phys.* **A 424** (1984) 525.
[GA84] GARRETA, D. *et al.*, *Phys. Lett.* **149B** (1984) 64.
[GA85] GARRETA, D. *et al.*, *Phys. Lett.* **151B** (1985) 473 (E).
[GA85a] GARRETA, D., in « Antinucleon- and Nucleon-Nucleus Interactions », eds. by G. E. Walker *et al.*, Plenum Publ., New York (1985).
[GA85b] GARRETA, D. *et al.*, *Phys. Lett.* **150B** (1985) 95.
[GA87] GALE, L. C., *Phys. Rev.* **C 36** (1987) 2152.
[GH74] GHESQUIÈRE, C., Proceedings of the Symposium of $\bar{N}N$ Annilation. Liblice. Ed. by L. Montanet. CERN 74-18 (1974) 436.
[GI86] GIBBS, W., Proceedings of Lake Louise Conference. Alberta, Canada (1986).
[GI86a] GIOVANNINI, A. and VAN HOVE, L., *Z. Phys.* **C 30** (1986) 391.
[GO85] GORRINGE, T. P. *et al.*, *Phys. Lett.* **162B** (1985) 71.
[GR76] GREGORY, P. *et al.*, *Nucl. Phys.* **B 102** (1976) 189.
[GR82] GREEN, A. M. and WYCECH, S., *Nucl. Phys.* **A 377** (1982) 441.
[GR83] GREEN, A. M., STEPIEN-RUDZKA, W. and WYCECH, S., *Nucl. Phys.* **A 399** (1983) 307.
[GR88] GREEN, A. M., in « The Elementary Structure of Matter ». Ed. by J. M. Richard *et al.*, Springer-Verlag, Berlin (1987) 190.
[GR88a] GREEN, A. M. and LIU, G. Q., Helsinki preprint HU-TFT-88-13 (1988).
[HA63] HAGEDORN, R., Relativistic Kinematics. Benjamin, Reading Mass. (1963) ch. 7.
[HA72] HAMER, C. J., *Il Nuovo Cim.* **A 12** (1972) 12.
[HA77] HAAK, J. F., *Phys. Lett.* **66B** (1977) 16.
[HA78] HAGEDORN, R. *et al.*, in « Hadronic Matter at Extreme Energy Density ». Erice (1978).
[HE85] HEISELBERG, H. *et al.*, *Nucl. Phys.* **A 446** (1985) 637.
[HE86] HERNANDEZ, E. and OSET, E., *Nucl. Phys.* **A 455** (1986) 584.
[HO88] HONG JUNG and MILLER, G. A., « The Elementary Structure of Matter ». Ed. by J. M. Richard *et al.*, Springer-Verlag, Berlin (1988) 259.
[IL82] ILJINOV, A. S., NAZARUK, V. I. and CHIGRINOV, S. E., *Nucl. Phys.* **A 382** (1982) 378.
[IN86] INGEMARSSON, A., *Nucl. Phys.* **A 454** (1986) 475.
[JA80] JAMINON, M., MAHAUX, C. and ROCHUS, P., *Phys. Rev.* **C 22** (1980) 2027.
[JA85] JANOUIN, S., thesis, unpublished.
[HA86] JANOUIN, S. *et al.*, *Nucl. Phys.* **A 451** (1986) 541.
[JA88] JASSELETTE, P., CUGNON, J. and VANDERMEULEN, J., *Nucl. Phys.* **A 484** (1988) 542.
[KA76] KAUFMANN, W. and PILKUHN, H., *Phys. Lett.* **62B** (1976) 165.
[KA84] KAHANA, S., Proceedings of the Workshop « Physics at LEAR », ed. by U. Gastaldi & R. Klapisch. Plenum Press, New York (1984) 485.
[KA85] KAUFMANN, W. *et al.*, *Phys. Rev.* **C 32** (1985) 1977.
[KA86] KANERT, W. *et al.*, *Phys. Rev. Lett.* **56** (1986) 2368.
[KL88] KLEMPT, E., in « Physics at LEAR with Low Energy Antiprotons », Harwood Acad. Publ., Chur (1988).
[KO86] KOHNO, M. and WEISE, W., *Nucl. Phys.* **A 454** (1986) 429.
[KÖ86] KÖHLER, T. *et al.*, *Phys. Lett.* **176B** (1986) 327.
[KO87] KO, C. M. and YUAN, R., *Phys. Lett.* **192B** (1987) 31.

[KU85] KUBO, K. I., TOKI, H. and IGARASHI, M., *Nucl. Phys.* **A 435** (1985) 708.
[LE74] LEON, M. and SEKI, R., *Phys. Lett.* **48B** (1974) 173.
[LE80] LEVMAN, G. *et al., Phys. Rev.* **D 21** (1980) 1.
[LE88] LEMAIRE, M. C. and CUGNON, J., to be published.
[LI88] LIPKIN, H. J., « The Elementary Structure of Matter ». Ed. by J. M. Richard *et al.,* Springer-Verlag, Berlin (1988) 24.
[Mc86] MCGAUGHEY, P. L. *et al., Phys. Rev. Lett.* **56** (1986) 2156.
[Mc86a] MCLERRAN, L. D., *Rev. Mod. Phys.* **58** (1986) 102.
[Mc86b] MCGAUGHEY, P. L., CLOVER, M. R. and Di GIACOMO, N. J., *Phys. Lett.* **166B** (1986) 264.
[MA76] MARGOLIS, B., MEGGS, W. J. and WEISS, N., *Phys. Rev.* **D 13** (1976) 2551.
[MA81] MARAYAMA, M. and UEDA, T., *Nucl. Phys.* **A 364** (1981) 297.
[MA83] MARAYAMA, M. and UEDA, T., *Phys. Lett.* **124B** (1983) 121.
[MA87] MARAYAMA, M. *et al., Nucl. Phys.* **A 473** (1987) 649.
[MA88] MARKIEL, W. *et al.,* TUM Preprint (1988).
[MA88a] MACHNER, H. *et al.,* to be published.
[MI84] MIYANO, K. *et al., Phys. Rev. lett.* **53** (1984) 1725.
[MO75] MONTANET, L. (1975), private communication.
[MÖ75] MÖHRING, H. *et al., Nucl. Phys.* **85B** (1975) 227.
[MO86] MOSER, E. F. *et al., Phys. Lett.* **179B** (1986) 25.
[MO86a] MOSER, E. F., Thesis, TUM, München (1986) unpublished.
[NA84] NAKAMURA, K. *et al., Phys. Rev. Lett.* **52** (1984) 731.
[NA85] NAKAMURA, K. *et al., Phys. rev.* **C 31** (1985) 853.
[NI76] NISHIMURA, H. and FUJITA, T., *Phys. Lett.* **60B** (1976) 413.
[NI83] NISKANEN, J. A. and GREEN, A. M., *Nucl. Phys.* **A 404** (1983) 495.
[NI85] NISKANEN, J. A. and MYRHER, F., *Phys. Lett.* **B 157** (1985) 247.
[OH73] OH, B. Y. *et al., Nucl. Phys.* **B 51** (1973) 57.
[OR73] ORFANIDIS, S. J. and RITTENBERG, V., *Nucl. Phys.* **B 59** (1973) 570.
[OS88] OSET, E., « Physics at LEAR with Low Energy Antiprotons ». Ed. by C. Amsler *et al.,* Harwood Acad. Publ., Chur (1988) 753.
[PH85] PHATAK, S. C. and SARMA, N., *Phys. Rev.* **C 31** (1985) 2113.
[PO56] PONTECORVO, B. M., *Zh. ETP* **30** (1956) 947.
[PO76] POVH, B., *Z. Phys.* **A 279** (1976) 159.
[PO85] POTH, H., Proc. Int. Symp. on Medium-Energy Nucleon and Antinucleon Scattering. Bad Honnef 1985. Ed. by H. V. von Geramb (Springer Lecture Notes in Physics, Berlin (1985), p. 357.
[PO86] POTH, H., Workshop on Antimatter Physics at Low Energy. Batavia, 1986 and CERN-EP/86-105.
[RA80] RAFELSKI, J., *Phys. Lett.* **91B** (1980) 281.
[RA82] RAFELSKI, J. and MÜLLER, B., *Phys. Rev. Lett.* **48** (1982) 1066.
[RA84] RAFELSKI, J., in « Physics at LEAR ». Ed. by U. Gastaldi and R. Klapisch. Plenum Press, New York (1984).
[RA88] RAFELSKI, J. in « Physics at LEAR with Low Energy Antiprotons ». Ed. by C. Amsler *et al.,* Harwood Acad. Publ., Chur (1988) addendum.
[RO75] ROY, J., Proceedings of the IV International Symposium on $\bar{N}N$ Interactions. Ed. by T. E. Kalogeropoulos and K. C. Wali. Syracuse Univ. (1975), p. III, 1.
[RO86] ROHMANN, D. *et al., Z. Phys.* **A 325** (1986) 261.
[RU66] RUBINSTEIN, H. R. and STERN, H., *Phys. Lett..* **21** (1966) 447.
[RU66a] RUDSTAM, G., *Z. Naturforschung* **21a** (1966) 1027.
[SA74] SATCHLER, G. R., Proceedings of the International Conference on Reactions Between Complex Nuclei. Ed. by R. L. Robinson *et al.,* North-Holland, Amsterdam (1974).

[SI88] SIMONS, L. M., Physics at LEAR with Low Energy Antiprotons. Ed. by C. Amsler *et al.,* Harwood Acad. Publ., Chur (1987) 703.
[SM88] SMITH, G. A., « The Elementary Structure of Matter », ed. by J. M. Richard *et al.,* Springer-Verlag, Berlin (1988) 197.
[ST79] STENBACKA, R. *et al.*, *Il Nuovo Cim.* **51A** (1979) 63.
[ST82] STROTTMAN, D., *Phys. Lett.* **119B** (1982) 39.
[ST84] STROTTMAN, D. and GIBBS, W. R., *Phys. Lett.* **149B** (1984) 288.
[SU84] SUZUKI, T. and NARUMI, H.., *Nucl. Phys.* **A 426** (1984) 413.
[TI84] TIMMERS, P. H., VAN DER SANDEN, W. A. and DE SWART, J. J., *Phys. Rev.* **D 29** (1984) 1928.
[TR61] TRUEMAN, T. L., *Nucl. Phys.* **6** (1961) 57.
[VA74] VANDERMEULEN, J., *Lett. Nuovo Cim.* **11** (1974) 243.
[VA80] VANDERMEULEN, J., *Lett. Nuovo Cim.* **28** (1980) 60.
[VA86] VANDERMEULEN, J., *Phys. Rev.* **C 33** (1986) 1101.
[VA88] VANDERMEULEN, J., *Z. Phys.* **C 37** (1988) 563.
[vo85] VON GERAMB, H., NAKANO, V. and RIKUS, L., *Lett. Nuovo Cim.* **42** (1985) 209.
[vo88] VON EGIDY, T. *et al.,* « Physics at LEAR with Low Energy Antiprotons ». Ed. by C. Amsler *et al.,* Harwood Acad. Publ., Chur (1988) 729.
[WO84] WONG, C. Y. *et al., Phys. Rev.* **C 29** (1985) 574.
[WY85] WYCECH, S., GREEN, A. M. and NISKANEN, J. A., *Phys. Lett.* **152B** (1985) 308.
[WY88] WYCECH, S. and GREEN, A. M., to be published.